Kitamura, Shuhei; Lagerlöf, Nils-Petter

Working Paper

Battles and capitals

ISER Discussion Paper, No. 1290

Provided in Cooperation with:
The Institute of Social and Economic Research (ISER), Osaka University

Suggested Citation: Kitamura, Shuhei; Lagerlöf, Nils-Petter (2025) : Battles and capitals, ISER Discussion Paper, No. 1290, Osaka University, Institute of Social and Economic Research (ISER), Osaka

This Version is available at:
https://hdl.handle.net/10419/331474

ISSN (Print) 0473-453X
Discussion Paper No. 1290
ISSN (Online) 2435-0982

BATTLES AND CAPITALS

Shuhei Kitamura
Nils-Petter Lagerlöf

June 2025

The Institute of Social and Economic Research
The University of Osaka
6-1 Mihogaoka, Ibaraki, Osaka 567-0047, Japan

Battles and Capitals*

Shuhei Kitamura† Nils-Petter Lagerlöf‡

June 20, 2025

*This paper replaces an earlier version titled Cities, Conflict, and Corridors. We are grateful for helpful comments from Hirokazu Ishise, Amrita Kulka, Nathan Nunn, and Yang Xie, as well as participants at the following conferences, workshops, and invited seminars: APEN Brisbane, EEA-ESEM Milan, GRIPS, Hitotsubashi, Keio, Kyoto, OEIO, SIOE Toronto, SWET, The BSE Summer Forum, The Tokyo Labor Economics Workshop, UEA London, ESAM Sydney, CEA Toronto, and ISER Osaka. Kitamura acknowledges financial support from JSPS (18K12768, 21K132840). Lagerlöf acknowledges financial support from the Social Sciences and Humanities Research Council of Canada (Grant No 435-2019-0701).

†ISER, Osaka University. E-mail: kitamura@iser.osaka-u.ac.jp.

‡Department of Economics, York University. E-mail: lagerlof@yorku.ca.

Abstract

The location of cities is linked to access to trade, but security also matters, in particular for capitals. Here we document this phenomenon, and explore its implications, in the context of Europe's Great Power era. First we show that Great Power battles tend to occur in shortest-distance corridors between belligerent powers' capitals, *except* where those corridors are intercepted by seas, mountains, and marshes. Then we show that capitals locate closer to each other when they have more of these types of geography between them. Finally, we show that city pairs are less likely to belong to the same state if they have more of this geography between them, allowing us to use geography to predict the territorial size and shape of Europe's Great Powers. In sum, our results suggest that terrain which slows down military incursions makes capitals safer, allowing them to locate closer to each other; given all capitals' locations, the surrounding geography then shapes the associated state territories.

Keywords: Conflict, battles, state fragmentation, cities

JEL codes: F52, H56, N43, N90

1 Introduction

> [A capital's] commercial and industrial importance is less than that of other cities in the same country, since the factors that influence the choice of site for a capital are often political and strategic rather than economic.
>
> *Spate (1942, p. 623)*

It is well understood that the location of cities is linked to access to trade, i.e., connectivity to other cities and/or natural resources. This has been shown in a recent and expanding literature, using data on geography, historical trade routes, archaeological sites, and more (see, e.g., Bleakley and Lin, 2012; Bosker and Buringh, 2017; Barjamovic et al., 2019; Bakker et al., 2021; Flückiger et al., 2024).

However, connectedness is not only, or always, beneficial for cities; security matters too, particularly for states' political centers, i.e., their capitals. As the above quote from the geographer Oskar Spate illustrates, this idea is not new. Bosker (2022, p.3) writes that capital cities are often located "in places further away from a [country's] borders or coastline that are less vulnerable from attack by foreign powers." Treivish (2016) argues that capitals tend to be farther from state boundaries compared to similarly sized non-capital cities. States have even on occasion moved their capitals in response to military threats, as when the Royal Government fled from London to Oxford during the English Civil War (Toynbee, 1970, Ch.6).

In this paper we revisit this idea and explore some interesting implications. We focus on the Great Power era in Europe, which was an environment with intense interstate competition, where threats to sovereign states come mostly from other states.

First we provide some suggestive evidence that Great Power capitals were indeed targeted by competitors. We use data from Kitamura (2021) on geo-coded Great Power battles and find that these tend to occur within 50 km wide shortest-distance corridors between the capitals of the belligerents. There is much weaker evidence that battles oc-

curred around state boundaries, or along corridors between the largest non-capital cities of the Great Powers involved.

However, we do find that battles tend to deviate from the shortest-distance corridor between capitals where it is intercepted by certain types of geography that were likely difficult for armies to cross: seas, mountains, and marshes; we discuss other geography variables as well, but these arguably make the most theoretical sense and also show the strongest correlations. Our interpretation is that these types of geography tend to extend the effective military distance between capitals at a given geodesic (direct-route) distance.[1] In other words, we interpret these types of geography as separating.

This should have implications for where capitals are located. Specifically, we argue (and illustrate in a model) that a more separating terrain should allow capitals to locate closer to each other. Intuitively, such terrain helps protect capitals from threats originating from other capitals, making shorter geodesic distances viable. For example, Paris and London may afford a shorter distance between them because of the English Channel, while, e.g., St Petersburg (or Moscow) may need longer distances to its potential enemies' capitals; consider, e.g., Napoleon's invasion of Russia in 1812. Moreover, we should expect to see less of that pattern for non-capital cities, for which security concerns do not carry the same weight.

To explore this, we use data on European city locations from Bosker et al. (2013) and look at pairs of capital cities in 1800, the latest year for which they provide data and also at the height of the Great Power era. We show that pairs of capitals tend to be geodesically closer when they have more of the same types of geography between them that we found affected battle locations, in particular seas and marshes (with some caveats for mountains, as discussed later).

This result indeed holds for pairs of capitals but not for pairs of non-capital cities, as we would expect if our theory is correct.

We also explore what implications this has for the size and shape of states. To do that,

[1] This interpretation is broadly consistent with a large body of work in military history on how geography shaped warfare and campaign routes; see, e.g., Engels (1978) on Alexander the Great and Collins (1998, Ch.1) for examples from modern times.

we look across all city pairs in 1800 (i.e., not only capitals). We find that the likelihood that both cities in a pair belonged to the same state 100 years later (i.e., in 1900, which is when Europe was the most unified) is lower when they have more of the same types of geography—seas, mountains, and marshland—between them. This is consistent with what we observed for capitals: if a more separating terrain allows capitals to locate closer, then such terrain should also be associated with more and smaller states within a given geodesic distance, since each sovereign state has exactly one capital.

This also allows us to predict the size and shape of European Great Power states, based on the locations of their capitals and the surrounding geography. In short, for each of city in the Bosker et al. (2013) data we compute the predicted probabilities of it belonging to the same state as different Great Power capitals and assign the city to the Great Power with highest predicted probability. We find similarities, but also interesting differences, between actual and predicted Great Power territories, which we think illustrate spatial variation in state capacity, and viability of state territories as they appeared in 1900.

The rest of this paper is organized as follows. Section 2 discusses some of the existing literature. Section 3 presents the data we use. Section 4 presents results referring to battle locations. Section 5 then analyzes geodesic distances between pairs of capitals and the likelihood that pairs of cities belong to the same state. A theoretical model is discussed informally in Section 6, with details deferred to an Online Appendix. Section 7 concludes.

2 Existing Literature

The topics discussed here relate broadly to research on the relationship between trade, war, borders, political unification, and development (e.g., Alesina and Spolaore, 2003; Rohner et al., 2013; Gancia et al., 2022; Schönholzer and Weese, 2022; Spolaore, 2023; Lipinski, 2024). One contribution relative to Alesina and Spolaore (2003) is that we study the location of capitals in relation to one another, rather than their own states' borders.

We also differ by focusing on how geography shapes state territories, which connects to an older debate about the link between Europe's specific geography and high degree of state fragmentation (see, e.g., Diamond, 1997; Jones, 2003; Hoffman, 2015; Ko et al., 2018;

Scheidel, 2019; Kitamura and Lagerlöf, 2020; Allen, 2023; Fernández-Villaverde et al., 2023; Weese, 2023). To test this hypothesis, earlier studies have explored the correlation between border locations and geography (Kitamura and Lagerlöf, 2020), or simulated quantifiable models of state expansion with geography as an input (Fernández-Villaverde et al., 2023). Other papers discuss the role of geography for conflict, but not for state fragmentation or the location of capitals (see, e.g., Jia, 2014; Iyigun et al., 2017; Dincecco et al., 2021, 2022, 2024).

One novelty with our empirical approach compared to all these is that we measure geography, and its effect, not where borders are located, or where battles occur, but across corridors between capitals. One motivation is that the locations of Great Power battles in European history have not related to local conditions as much as traversing armies crossing paths there.

Our "corridor" approach may have something in common with work on how spatial proximity affects interstate conflict (e.g., Gleditsch and Singer, 1975; Bremer, 1992). More recently, Spolaore and Wacziarg (2016) explore other distance measures (in particular genetic distances), finding that geodesic distances are negatively correlated with interstate conflict, also with various other distance controls. However, none of these papers explores where conflict occurs spatially or interacts with geography.

A large literature examines how geography affects the locations of modern cities, and economic activity more generally. Examples include coastlines (Rappaport and Sachs, 2003; Michaels and Rauch, 2018), portage sites (Bleakley and Lin, 2012), and land productivity (Henderson et al., 2018), as well as proximate historical factors that might fundamentally depend on geography, e.g., the early emergence of statehood (Cook, 2024) and agriculture (Dickens and Lagerlöf, 2023), and historical population density (Maloney and Valencia Caicedo, 2016). We differ from these in our focus on how geography can impact military security.

The theoretical links between security and the emergence of cities are explored by Dal Bó et al. (2022), but not specifically in regard to capitals. Dincecco and Onorato (2016) study the effect of battles on city growth, but not what determines battle locations, state territories, or the location of capitals.

3 Data

3.1 The Battle Data

Our starting point for the empirical analysis is a new battle dataset compiled by Kitamura (2021). Most of it originates from Wikidata and Wikipedia.[2] This source material changes over time, but according to Kitamura (2021) edits to the information used here (i.e., years and locations) tend to be few and minor.

The full dataset contains information about, e.g., start and end years of battles, their geo-coordinates, and lists of belligerent powers on different sides of the battle.[3] Although it covers battles throughout human history and across the world, we focus on Europe and an era in which regular Great Power (GP) conflicts shaped its political geography. To that end, we consider all battles with geo-coordinates within a rectangle with its northwestern and southeastern corners in Reykjavík and Baghdad, respectively. Temporally, we initially restrict attention to battles with a start year from 1525 (the birth of Prussia) up to and including 1913, to avoid battles from World War I and onward, when new technologies likely altered the impact of geography on warfare. Choosing 1913 as the exact end point is not important, as explained below. We discuss separately what we can learn from the period 1914-1945.

Our interest is on battles involving the major historical GP states in Europe. Obviously, the identities, names, regimes, and territories of these powers have changed over time. For example, one GP has been known as England, Great Britain, and the United Kingdom (of Great Britain and Ireland) at different points in history. Germany and Prussia have intertwined histories, the latter being (a dominant) part of the former when the German Empire was created in 1871.

Here we consider the following seven GPs: England/Great Britain; France; Russia;

[2]There are other papers using Wikidata and Wikipedia for different applications (see, e.g., Laouenan et al., 2022, who study notable people in human history), but to the best of our knowledge Kitamura (2021) is the first to compile data on battles using this source.

[3]The dataset also contains information on outcomes of battles (who won or lost, etc.), but we do not use that information here.

Prussia/Germany; Austria/Habsburg Empire/Austria-Hungary; Spain; and the Ottoman Empire. These are the ones discussed in most detail in the influential study of the European Great Power system by Levy (1983).[4] The matching of battles to GPs was done manually by Kitamura (2021), who provides further details on this process.

These GPs also had relatively stable capital locations, with two exceptions: Moscow was the Russian capital before 1712 and after 1917, and 1728-1730, and St Petersburg otherwise; Königsberg (Kaliningrad) was the capital of Prussia before 1701 and Berlin after. We return to these changes in capitals below.

Since corridors can be constructed only between different Great Power capitals, we do not include battles where the same state (by our definition) was the only belligerent involved, i.e., on both sides of the battle. This avoids most civil war battles, except those where another GP was involved on one side of the battle (primarily during the English Civil War and the French Revolution).

We also ignore battles with imprecise location data. The typical example is a battle somewhere along a river or valley, where the sources do not specify which part (see Kitamura, 2021, for further details).

We include naval battles in the benchmark analysis, but the results are robust to dropping these (see Section A.2 of the Online Appendix). It arguably makes sense to include naval battles, since a negative effect of sea on the likelihood of battle might otherwise seem obvious.

The seven GPs can form 21 pairs in total, but some of these fought no, or very few, battles over the period considered. In our benchmark analysis, we drop those pairs which fought fewer than ten battles, leaving eleven pairs in total. This serves partly to focus on Great Power pairs that were in regular and long-lasting conflict. Section A.2.4 of the Online Appendix presents results based on all 21 pairs.

Considering only pairs that fought at least ten battles also ensures that we include almost no battles involving Russia or Prussia when they had Moscow and Königsberg,

[4]Three more European states that were defined as Great Powers by Levy (1983) are ignored here, namely Sweden, Italy, and the Netherlands. However, these were not GPs over nearly as long periods of time as the other seven; see Levy (1983, Table 2.1).

respectively, as capitals.[5] That is, treating St Petersburg and Berlin as the capitals of Russia or Germany/Prussia makes sense with this restriction.[6] More generally, even though their territories and regimes were often fluid, we can think of these seven GPs as having relatively fixed political centers, at least at times when they were involved in conflict.

The upshot is a set of 684 battles fought between these eleven different pairs of GPs, starting with the Battle of Pavia in 1525 and ending with the Battle of Plovdiv (or Battle of Philippopolis) in 1878. In other words, although we chose 1913 as the end point, this choice in not too important, since these GPs did not fight each other in the European theatre after 1878 until the start of World War I.

3.1.1 Cell Data

We measure the occurrence of battles across space by dividing the rectangular area considered (with corners in Reykjavík and Baghdad) into cells of equal size, with sides of one degree latitude and longitude.

We want our results not to be based on cells in the extreme periphery of Europe, where no battles are likely to be fought, so we drop all cells north of the most northerly cell in which battles took place between any of the eleven pairs, and cells south of the most southerly such cell, etc. This leaves us with 1,450 cells in total. For each cell, we can measure the number of battles fought between each of the eleven GP pairs.

All in all, this gives us a dataset with $11 \times 1,450 = 15,950$ observations, where the unit of observation is a combination of a GP pair and a cell. The outcome of interest in the battle analysis is an indicator for whether a cell had any battles, or not, involving the relevant GP pair. Although there is no time variation, the data structure is panel-like, in the sense that it displays variation across both cells and GP pairs; for example, a cell could record battles between England and France, but not between France and Spain, or

[5]The single exception is the Battle of Turckheim in 1675, involving Prussia and France, which we drop separately, since Königsberg was the capital. This has no meaningful effect on the results.

[6]Berlin would probably have been a more important power center than Königsberg ever was. The choice between Moscow and St Petersburg might be less obvious (note, e.g., that Napoleon's 1812 invasion of Russia targeted Moscow), but assigning Moscow as capital instead of St Petersburg does not change the results much; see Section Section A.2.4 of the Online Appendix.

England and Spain.

Figure 1 shows a map of the precise battle locations and which cells are coded as battle cells for at least one GP pair.

3.2 Geography and Shortest-Distance Corridor

The variable that we call the *Shortest-Distance corridor* (SD corridor, for short) is an indicator for cells intersected by a 50 km buffer zone around the shortest-distance line between the relevant pair of capitals. This line takes into account the curvature of the Earth, so it does not look like a straight line on a projected map.

Different segments of a SD corridor may of course have different access to roads, ports, and rest stops. However, such factors seem endogenous and probably changed over time (and across seasons); for example, railways began to matter later in our study period. Moreover, troops need not necessarily follow roads but could often travel across open fields or frozen waterways, and absent geographical obstacles the most cost efficient path should be the shortest route. Our approach is to use geography data to capture factors that we believe may have forced deviations from that route.

We consider three geography variables. Most obviously, mountains and marshland must have been more difficult to cross with cavalry and cannons. The case for seas is less obvious, as civilian transport is often easier by ship than on land. However, troops can access food and water more easily on land, and loading/unloading military material onto/from a ship can be risky and time consuming; Armadas can often be spotted at long distances.

Given our choice of geography variables, we use the following sources. Marshland data are from the Global Lakes and Wetlands Database maintained by the World Wildlife Foundation (linked to here; Level 3, Categories 4 and 5). We use a relatively broad definition, including freshwater marshes, floodplain and swamp forest, and flooded forest. The binary cell-level variable is an indicator of whether a cell is intersected by anyone of those types of marshes.

To define mountains we use elevation data from NOAA National Centers for Environ-

mental Information (linked to here). A cell is defined as having a mountain when its mean elevation exceeds 800 meters, with alternative cutoffs explored in the Online Appendix.

We define sea as the absence of land, using data from GADM. The sea indicator equals one when a cell is intersected by sea, i.e., not fully covered by land.

Figure 2 illustrates the battle cells for six GP pairs, together with the associated shortest-distance corridors, and cells where each of the three geography variables are present.

Table A.1 in the Online Appendix presents summary statistics for the main variables used in the battle analysis.

3.3 City and State Data

The city data are from Bosker et al. (2013), who provide information on multiple European cities at the turns of the centuries from 800 CE to 1800 CE. City population is reported for city-years when they exceed 5,000. The dataset also contains geo-coordinates, as well as information about which cities were capitals at different points in time.

The spatial coverage is approximately Europe and surrounding areas, such as North Africa and parts of Near East.

Our benchmark analysis in Section 5 considers cities with a population above 5,000 in 1800 CE, with some robustness checks in the Online Appendix. We choose the year 1800 because it is the latest available in Bosker et al. (2013). The unit of analysis is a pair of (capital) cities, with geography measured across buffer zones around the shortest-distance line between cities (or capitals).

The sources for the geography variables are the same as for the cell-level data (see Section 3.2 above), except that we here measure sea using Natural Earth. Different from the cell-level analysis, where we constructed binary indicators, we here use the *fraction* of the relevant buffer zone covered by mountains, marshland, and sea. This makes more sense in this context, since the corridors are so much larger geographical areas than the cells.

Data on state borders are from Euratlas (Nüssli, 2010). These contain geospatial information on the borders of sovereign states in Europe and surrounding areas at the turn of

the centuries from 1 CE to 2000 CE. We use these data to determine which pairs of cities belonged to the same sovereign state. The benchmark analysis considers state borders in 1900 based on Euratlas, while the Online Appendix explores other years and data sources.

Table A.17 in the Online Appendix presents summary statistics for the main variables used in the city data analysis.

4 Battle Data Analysis

For the battle-level analysis the unit of observation is a one-degree cell. We consider cells both with and without battles, thus allowing us to use information about locations that did not see any battles. For each cell we measure if there were any battles fought there during the period of interest and involving the GPs under consideration.

More precisely, our main outcome variable is an indicator variable denoted $B_{i,p}$, taking the value one if a battle between pair p occurred in cell i over the benchmark period (1525-1913), and zero otherwise. (Section A.2 of the Online Appendix considers an intensive-margin measure as the outcome variable, i.e., the number of battles rather than a battle indicator.)

Our independent variables of interest include three geography variables, all binary indicators. $H_{800,i}$ equals one if average elevation in cell i exceeds 800 meters above the sea, and zero otherwise. (We consider different heights in Section A.2.) M_i is an indicator for a marsh (or swamp) intersecting cell i. S_i indicates whether the cell is intersected by sea.

The remaining variable of interest is the shortest-distance corridor. Like the geography variables, this is also a binary indicator, and denoted by $D_{i,p}$. Note that $D_{i,p}$ varies both across cells and GP pairs.[7]

[7]For example, if p refers to the pair England-France, and cell i intersects with the shortest-distance corridor between London and Paris, then $D_{i,p} = 1$, while $D_{j,p} = 0$ for cells $j \neq i$ off the London-Paris corridor, and $D_{i,q} = 0$ for all GP pairs $q \neq p$, whose corridors do not cover cell i.

4.1 Direct Effects

We are going to present results from a few different regression specifications. Consider first this:

$$B_{i,p} = \alpha + \beta_{\mathrm{D}} D_{i,p} + \lambda_{\mathrm{S}} S_i + \lambda_{\mathrm{H}} H_{800,i} + \lambda_{\mathrm{M}} M_i + \omega_p + \varepsilon_{i,p}, \tag{1}$$

where ω_p is a GP pair fixed effect, and $\varepsilon_{i,p}$ is an error term. If $\widehat{\beta}_{\mathrm{D}} > 0$, then battles tend to happen more often in cells along the shortest-distance corridor than elsewhere.

The first three columns of Table 1 bear this out. In column (1) we consider a specification without any geography controls or fixed effects; column (2) adds geography controls; and column (3) adds both geography controls and pair fixed effects. Throughout $\widehat{\beta}_{\mathrm{D}}$ comes out as positive and significant. We also note that all three geography measures carry negative coefficients, suggesting that battles tend to occur on land, and in terrain that is not too mountainous or marshy. However, these direct effects are hard to interpret, since geography can vary with, e.g., distance from the corridor.

We can also add cell fixed effects to the formulation in (1), absorbing the geography controls, and giving us the following specification:

$$B_{i,p} = \beta_{\mathrm{D}} D_{i,p} + \omega_p + \gamma_i + \varepsilon_{i,p}, \tag{2}$$

where γ_i capture the cell fixed effects. This is estimated in column (4) of Table 1, again showing us $\widehat{\beta}_{\mathrm{D}} > 0$.

One possibility is that the positive coefficient on the shortest distance corridor merely captures an effect from cells far away from the belligerent states, in regions where they had no reason to fight. To address this, columns (5) and (6) of Table 1 consider the same specifications as in columns (3) and (4), but restrict the sample to cells within 300 km of the shortest-distance corridor. This shrinks the sample to about 10% of its original size. While the estimated coefficient of interest shrinks in magnitude, it remains positive and significant.

Finally, column (7) of Table 1 considers the same specification as in column (4), but allows standard errors to be clustered at the pair and cell level. The corridor indicator becomes slightly less precisely estimated, but remains significant at the 5% level.

4.2 Interaction Effects

So far we have documented that GPs tend to fight more battles along their shortest-distance corridors. Next we examine if our measures of geography tend to push battles off that corridor. To that end, we estimate the following regression equation:

$$\begin{aligned} B_{i,p} = \quad & \beta_{\mathrm{D}} D_{i,p} \\ & + \beta_{\mathrm{S}} D_{i,p} S_i \\ & + \beta_{\mathrm{H},800} D_{i,p} H_{800,i} \\ & + \beta_{\mathrm{M}} D_{i,p} M_i \\ & + \omega_p + \gamma_i + \varepsilon_{i,p}, \end{aligned} \tag{3}$$

where, as before, ω_p and γ_i are fixed effects for GP-pair and cell, respectively, and $\varepsilon_{i,p}$ is an error term. As earlier, we expect $\widehat{\beta}_{\mathrm{D}} > 0$. Now we should also expect $\widehat{\beta}_{\mathrm{S}} < 0$, $\widehat{\beta}_{\mathrm{H},800} < 0$, and $\widehat{\beta}_{\mathrm{M}} < 0$. As discussed above, we might expect this geography effect to be present in all cells, not only along the corridor, but any such effects are absorbed by the cell fixed effects.

In other words, we expect seas, marshes, and mountains to make the hypothesized path of military advance deviate from the shortest route. If this is the case, it suggests that these geographical characteristics increase the effective military distance between the two GPs political centers, at given geodesic distance.

Table 2 considers a few different regressions involving these interaction effects. Columns (1)-(3) show the results from three separate regressions, where the independent variables include the indicator for cells on the shortest-distance corridor, and each of the three geography variables and their interactions with the shortest-distance corridor, entered one at a time. The interaction effects all come out as negative, although not significant for marshes. Column (4) enters them all together and now the coefficients on the interaction terms become precisely estimated, all three being significantly different from zero at the 5% level, or lower. This holds also when entering GP pair fixed effects in column (5), and with both pair and cell fixed effects in column (6); note that the direct geography effects are dropped in column (6), as they are absorbed by the cell fixed effects. Column (7) uses the same fixed-effects specification as in column (6), but allows standard errors to be clus-

tered at the pair and cell level. This renders the coefficient on marshes insignificant, but seas and mountains still come out as significant at the 5% level.

Overall, this supports the idea that these types of geography tend to push battles off the shortest-distance corridor, on which battles would otherwise tend to be fought, the result being a longer effective distance between the capitals.

Figure 3 illustrates how the means of the different geography variables vary between observations (cell-GP pairs) with and without battles, both for the full sample and for observations on the shortest-distance corridor between the belligerents' capitals. This shows that geography indeed differs between observations with and without battles, in particular when we consider cell/pairs on the corridor. In other words, these types of geography do push battles off the corridor.

4.3 Robustness

4.3.1 Alternative Corridors

Section A.2 of the Online Appendix pursues several robustness checks of the main results from our battle analysis. First, to assess if our results are truly about corridors between capitals we consider two alternative corridors. One runs around the territorial contours of the Great Powers; the other between the largest non-capital cities, which we chose to be Barcelona, Budapest, Izmir/Smyrna, Manchester, Marseilles, and Moscow (for motivation of these choices see Section A.2.2). Maps of these alternative corridors for different Great Power pairs are shown in Figures A.6 and A.7.

Both these alternative corridor measures show positive and significant correlation with the battle indicator when added as controls to the regressions in Table 1 (see Tables A.3 to A.6). However, the coefficients on our benchmark corridor measure always come out as larger and more significant than the other two, and similar in size to our benchmark regressions in Table 1. This holds also when we restrict the sample to cells close to the benchmark corridor. In other words, our findings do not seem spurious.

4.3.2 Alternative Geography Measures

Section A.2.3 in the Online Appendix explores how the results in Table 2 change when using some alternative geography variables, namely indicators for rivers, lakes, and high levels of agricultural suitability, the last one based on data from Galor and Özak (2016). Of these three, only the river indicator comes out as significant when interacted with the SD-corridor, but with a positive sign. In other words, there is no evidence from our battle data that rivers are obstacles—like seas, mountains, and marshes appear to be—but rather the opposite. This is maybe not too surprising, since the effect of rivers can be theoretically ambiguous. As discussed in Pounds (1972, , Ch. 11) and Kitamura and Lagerlöf (2020), rivers can serve as borders between states, but also unify by facilitating transportation. Similarly, rivers can supply water for troops on campaign, while in some cases also being difficult to cross. For the rest of this paper, we focus our analysis on the three benchmark variables that we feel make most sense as geographical obstacles to military mobility.

4.3.3 Further Robustness Checks

Section A.2.4 of the Online Appendix considers several other robustness checks of the results in Table 2, e.g., adding city interactions, dropping battles close to capitals, letting Moscow be the capital of Russia (instead of St Petersburg), dropping sea battles, using the number of battles (rather than a battle dummy) as the dependent variable, and allowing for spatially correlated standard errors. None of these changes alters the results much, at least not in ways suggesting that the correlations of interest are spurious; in some cases the results rather strengthen.

One thing that does weaken the results is measuring battle outcomes over a later period, 1914-1945. However, this finding arguably makes sense, since advances in transport and military technologies at some point should make geography less of an obstacle for advancing armies. It is also consistent with how new modes of transport, such as railroads and steam ships, affected the spatial distribution of economic activity (see, e.g., Delventhal, 2018; Ellingsen, 2025; Nagy, 2023).

5 City Data Analysis

The analysis so far suggests that certain types of geography tend to push battles off the shortest-distance corridor between the belligerents' capitals. Our suggested interpretation is that these types of geography increase the effective military distance between the capitals.

This need not be interpreted too literally. We do not have in mind any specific military campaign that aimed for a particular capital, and detoured around mountains, seas, or marches. Such examples may exist, but we imagine a more long-run and indirect chain of causation. For example, armies may aim for certain non-capital cities or locations whose military-strategic relevance stem from a belligerent's capital being easier to reach from there, in turn making them more important to defend, and thus a more likely to become battle locations.

In this section, we look at city data for patterns that are consistent with the idea that geography affects the effective distances between capitals. First, we examine if the geodesic distances between pairs of capitals tend be shorter when the geography between them is more separating. We would expect this to be the case, because a more separating terrain should afford capitals to be closer. Put another way, terrain that is easier to traverse requires longer distances between capitals for the states' long-run survival.

Second, we ask if pairs of locations (cities) are more likely to belong to different states when they have a more separating terrain between them. This is based on the same reasoning as above, since shorter distances between capitals should imply smaller states.

Section 6 below discusses a theoretical framework that formalizes this intuition.

5.1 Geodesic Distances Between Capitals

To examine geodesic distances between capitals, we use data from Bosker et al. (2013), and look at pairs of capital cities in 1800. We also add the Russian capital of St Petersburg, to get a little closer to our battle data, but results are not sensitive to this inclusion.

We then run a few regressions where the dependent variable is the geodesic distance

between the capitals, or the length of the corridor, denoted $L_{i,j}$. The three independent variables of interest correspond to those used in our earlier battle analysis: the fraction mountain (with elevation above 800 m), $H_{800,i,j}$; the fraction sea $S_{i,j}$; and the fraction marsh, $M_{i,j}$. These are all measured as fractions across a corridor's total area (the 50 km buffer zones around then shortest-distance line). The regression equation can be written:

$$L_{i,j} = \delta_{\mathrm{S}} S_{i,j} + \delta_{\mathrm{H},800} H_{800,i,j} + \delta_{\mathrm{M}} M_{i,j} + \eta_i + \eta_j + \varepsilon_{i,j}, \tag{4}$$

where η_i and η_j denote city fixed effects, one for each of the capital cities in the pair.[8] These fixed effects absorb anything that directly affects distances for any particular capital and/or its location, and follows the approach of Spolaore and Wacziarg (2006) (see also Spolaore and Wacziarg, 2009, Footnote 42).

We expect the estimates of the different δ's to be negative. Columns (1) and (3) in Table 3 present results from two regressions that bear this out: larger fractions sea or marshland along the corridors are associated with shorter geodesic distances, with the estimated coefficients being negative and highly significant. This suggests that a more separating terrain tends to pull the capitals closer to each other.

The coefficient on the fraction mountain in column (2) carries the wrong sign, and also comes out as highly significant. However, when all three geography variables enter together in column (4), the coefficient on the fraction mountain shrinks in absolute magnitude and becomes less precisely estimated, while the corresponding coefficients on the fractions sea and marshland become larger in absolute terms.

Moreover, the negative estimate of the mountain coefficient is not robust. Column (5) drops those pairs where both cities were capitals only in 1800, and became non-capital cities in either 1900, 2000, or in recent modern times (according to Euratlas and GADM, respectively; see below). These cities are Firenze, Genoa, Milano, Naples, and Turin in modern Italy and Munich in modern Germany; note that Italy and Germany did not exist as states in 1800. As seen in column (5), when dropping these pairs, thus shrinking the

[8] More precisely, let $\eta_i\phi_i + \eta_j\phi_j$ be two terms in the sum $\sum_{k=1}^{N} \eta_k\phi_k$, where N is the number of capitals (or number of cities), and η_k is the coefficient on the dummy variable for capital k, denoted ϕ_k. This dummy is such that $\phi_k = 1$ if $i = k$ or $j = k$, and $\phi_k = 0$ otherwise. The two terms (and the whole sum) thus equal $\eta_i\phi_i + \eta_j\phi_j = \eta_i + \eta_j$ for capital cities i and j.

sample by about 4%, the coefficient on the fraction mountain is no longer significantly different from zero.

Rather than looking at each type of geography in isolation we can consider a composite measure that we call a *Separatedness Index*, constructed as this weighted average of the three geography variables:

$$.162 \times S_{i,j} + .166 \times H_{800,i,j} + .13 \times M_{i,j}. \tag{5}$$

The weights are given by the estimated coefficients on the interaction terms in column (5) of Table 2. These capture to what degree the presence of each type of geography tends to push battles off the shortest distance corridor, thus extending the effective distance.[9] The coefficient on this index is negative and significant in column (6) of Table 3, consistent with our theory: capitals tend to be geodesically closer to each other when they have more separating geography between them.

Finally, columns (7) and (8) present result based on the same specifications as in (4) and (6), but with standard errors clustered on pairs of 5×5 degree cells.[10] The estimates stay significant.

In sum, a more separating geography seems to be associated with shorter geodesic distances between pairs of capitals.

5.1.1 Robustness and Mechanisms

In Section A.3 of the Online Appendix we present results that inform us further about the mechanisms involved. First, we consider pairs of non-capital cities, without finding any negative correlations like those which we find for pairs of capitals in Table 3. If anything, the correlations for non-capitals tend to be positive. In other words, there is something specific about capitals that makes them different from other cities.

We also restrict the sample to pairs of particularly large cities, as measured by population. This could be of interest because capitals tend to be larger than other cities, suggest-

[9] Since the weights in (5) are similar in size an equal-weighted average produces similar results.

[10] That is, we divide the map into cells centered on degrees latitude and longitude divisible by 5. Each pair of capitals (or cities) belongs to one unique cell pair and we cluster the standard errors on such cell pairs.

ing that size itself might drive these patterns.[11] Again, we find no significant relationship between distances and separatedness for large non-capitals, while we do find it for large capitals.

We also explore some alternative interpretations of what constitutes a capital, and thus the type of sovereign state of which it is the center of power, by restricting the sample to capitals of Great Powers only, considering two different definitions. This shrinks the sample a great deal, but we still find negative, and mostly significant, correlations.

Overall, we believe this lends support to our suggested interpretation about why a separating geography leads to shorter distances between capitals: it is more important for capitals than for other cities to be out of reach of competing powers' armies; therefore, a more separating terrain, that is harder to cross, affords shorter geodesic distances.

5.2 Same-State Outcomes

Next we explore if pairs of cities are more likely to belong to different states when they have a more separating terrain between them. We could do this exercise for arbitrary pairs of locations, e.g., cells, but because state territories have a more meaningful interpretation in regions that are more densely populated (or populated at all), we choose pairs of cities.

To that end, we again use the city data from Bosker et al. (2013), and the year 1800 CE, but consider all cities with a population above 5,000 (i.e., not only capitals). We want to know if these were more likely to belong to different states if the geography between them was more separating controlling for the geodesic distance between them.

As in the analysis of capital pairs above, we use the geo-coordinates of cities to find the shortest-distance line between city pairs and measure the same types of geography as in our earlier analysis across 50 km buffer zones from the shortest-distance line. As before, we refer to these as corridors between cities.

Also in line with the capital-pairs analysis, we focus on 1800 CE, the latest year for which Bosker et al. (2013) report data. Same-state outcomes are based on Euratlas borders

[11] Larger cities may be more likely to become capitals, and capitals may also grow faster than other cities. For an example of the latter, see, e.g., Kulka and Smith (2024), who finds that US cities grow faster when becoming county seats.

of independent states in 1900, a century after we measure cities. This is when the number of states in Europe was at its lowest (see, e.g., Gancia et al., 2022, Table 1), and also a point in time when the states that we considered in our battle analysis formally existed, in particular Italy and Germany.

Excluding cities outside Euratlas state territories in 1900, this gives us 241,860 city pairs.

Let the outcome variable be an indicator denoted $C_{i,j}$, taking the value one if the two cities i and j belonged to the same state (in 1900, the year when we measure outcomes), and zero otherwise. Using the same notation as earlier for the remaining variables, we can now write the regression equation as

$$C_{i,j} = \lambda_{\mathrm{L}} L_{i,j} + \lambda_{\mathrm{S}} S_{i,j} + \lambda_{\mathrm{H},800} H_{800,i,j} + \lambda_{\mathrm{M}} M_{i,j} + \eta_i + \eta_j + \varepsilon_{i,j}, \tag{6}$$

where the terms η_i and η_j represent the same type of fixed effects as in (4), although referring to all cities (not only capitals). These absorb anything that varies at the city level.

We are interested in the estimates of the different λ's, which we all expect to carry negative signs. That is, any two cities should be less likely to belong to the same state if they are farther from each other and if they are more separated by seas, mountains, or marshes. Put another way, they should be more likely to belong to the same state if they lie close to each other, with flat, non-marshy dry land between them.

Table 4 presents least-squares estimates from various specifications similar to that in (6), letting the different geography variables enter both one by one and together.

The signs come out the expected way, and highly significant, when all geography controls enter together in column (4). The same is true when entering the fraction sea or the fraction mountain separately in columns (1) and (2). The significant and positive effect when entering the fraction marshes separately in column (3) is an anomaly, but (as mentioned) this result reverses when entering all geography variables together in column (4). We also see that the inclusion of the fraction marshes increases the size of the estimated coefficients on the other two geography variables, suggesting that these variables capture different dimensions of the separating effects of geography. Notably, the marshes variable has a negative correlation with the other two, as swampy areas tend to be located on

land and at low elevation.

Column (5) uses the Separatedness Index, defined in (5), in lieu of the three geography variables. The index comes out as negative and significant at the 1% level.

Columns (6) and (7) cluster the standard errors on cell pairs (same as in Table 3), with similar results as in columns (4) and (5), except that the fraction marshes comes out as significant only at the 10% level in column (6).

Section A.4 of the Online Appendix makes several robustness checks of the results in Table 4. First, we explore if the results hinge on using 1900 as the outcome year, a point in time when Europe was at its most unified. We find that they are not. Letting the same-state dummy be defined on state borders in later years than 1900 the results are almost identical.

We also consider pairs of cities that existed earlier than 1800. This could be important if we believe that some cities emerged simultaneously and/or endogenously with states. However, when using pairs of cities that existed in 800 CE already—preceding modern European state formation by a few centuries, and the earliest year for which Bosker et al. (2013) have data—the results are similar to those in Table 4.

5.2.1 Predicted Great Power Territories

We can use the same-state regressions to make predictions about state territories. To keep close to our city-level analysis, we here think of the territory of a Great Power as the set of cities that are most likely to belong to the same state as its capital: London, Paris, Madrid, Berlin, Vienna and Istanbul. We ignore Russia and St Petersburg, since Bosker et al. (2013) do not have data on Russian cities. We also arbitrarily assume that cities belong to none of these Great Powers if the highest predicted probability across all of them falls below 0.15; see further discussion below.

The results are shown in the map in Figure 4, where actual state borders are also indicated. We can make several observations. First, the predicted Great Power territories are not circular or oval, as we would expect if only geodesic distance mattered; deviations from such shapes illustrate the role of geography for these predictions.

Second, the fits are imperfect in ways that are insightful. For example, the Ottoman

Empire is much larger than its actual territory in 1900, stretching into the Balkans and Sicily, but that fit becomes better if we use the actual territory in 1800 instead; see Figure A.10 in the Online Appendix. This may also speak to why modern Turkey's capital is in Ankara.

Another example is the prediction for France, which does not reach the south, or the Mediterranean coast, of the country as it looked in 1900 (or today). However, some of these areas (e.g., Nice and the Duchy of Savoy) were not always part of France before then. Note also that Monaco remains an independent state to this day.

Third, the cities/regions that are predicted to not belong to any Great Power are located in regions stretching from the Benelux countries, across the Alps, and into Italy. This is where we see many small states in 1900, and often to this day; note that Italy was not unified until 1861. As mentioned, we set 0.15 as the predicted probability threshold below which cities are assumed to not belong to any Great Power. This number is arbitrary, but we chose it to allow the map to match these broad patterns. For comparison, Figures A.11 and A.12 in the Online Appendix show the results when instead using 0.1 and 0.2 as thresholds, producing a worse match with these broad empirical patterns.

Section A.4.1 in the Online Appendix also explores quantitatively how well the predicted territories compare to the actual, according to what we call the overlap ratio. This ranges from zero, when there is no overlap between predicted and actual territories, to one, when there is perfect overlap. In our predictions, this overlap ratio ranges from .46 for Austria-Hungary to .96 for England.

Interestingly, if we change the capitals to the alternative cities used in Section 4.3.1, considering each Great Power at a time and keeping the capitals of the other Great Powers fixed, then the overlap ratios tend to fall. The one exception is Austria-Hungary, where the overlap ratio is higher with Budapest as capital instead of Vienna. Although the picture is somewhat mixed, we think this is suggestive of a pattern where Great Power capitals tend to be positioned such that they are well connected to their own territories, but not those of their competitors. For example, when using Marseilles as capital of France instead of Paris, its predicted territory shows little semblance to its actual (see Online Appendix Figure A.14).

6 Theoretical Framework

We have already discussed our preferred interpretation of our findings. To make this a little more concrete, Section A.1 of the Online Appendix suggests a simple but useful model that can help us think about the underlying mechanics.

In the model, the effective distance between two locations depends both on how far they are from each other in a geodesic sense and on the terrain between them, which varies across space. Terrain that is more separating (i.e., harder to cross) produces a greater effective distance for a given geodesic distance.

States (or their elites) place their capitals to maximize the effective distance to their closest neighbors' capitals. Assuming that borders are located geodesically half-way between capitals, the model then gives us state territories. Given these territories, we assume that each state has one non-capital city located at the point within its territory that has the lowest separatedness, meant to capture the broad idea that non-capital cities gain from being well connected. (Alternatively, they may locate where land productivity is high, associated with a less separating terrain.)

We then simulate the model 5,000 times, each with a different randomly generated geography. We find that capitals are always located geodesically closer where the terrain is more separating, while the same does not hold for non-capital cities. (See Figure A.5 in the Online Appendix.) Intuitively, for non-capital cities two effects pull in opposite directions: because each state has one non-capital city, there are more such cities where there are more states, i.e., where the terrain is more separating; on the other hand, within states, non-capitals locate where separatedness is low. The contrasting patterns for capitals and non-capitals are consistent with the findings discussed in Section 5.1.

A corollary finding to capitals being geodesically closer where the terrain is more separating, and states' territorial borders being located between capitals, is that any two locations are less likely to belong to the same state in places that have more separating terrain. This matches our findings in Section 5.2.

7 Conclusion

While cities tend to locate where they are well connected for the purpose of trade, they also need to stay safe from enemies. This is particularly true for capitals.

In this paper we use this insight, together with data on battles and cities in Europe, to explore how geography has influenced the locations of battles and capitals and thereby the territorial size and shape of states. The focus is on the Great Power era.

We first document that capitals appear to have been (directly or indirectly) targeted in military conflicts between European Great Powers. To that end, we use data from Kitamura (2021) on geo-coded battles to document that these tend to occur within shortest-distance corridors running between the capitals of the belligerent powers. However, we also show that battles tend to deviate from that corridor where it is intercepted by certain types of geography, specifically seas, mountains, and marshes. These results are robust to various controls, sample restrictions, econometric specifications, and alternative definitions of variables. Our interpretation is that these types of geography have served as obstacles for armies, and thus tended to make capitals safer. In other words, they tend to extend the effective military distances between capitals for a given geodesic distance.

We argue that one implication of this finding is that areas with more separating terrain should have more and smaller states, with capitals located closer to each other. To test this we use city data from Bosker et al. (2013), and find that capitals tend to be geodesically closer to each other when they have more of these types of geography between them, in particular more sea and marshland, with the results for mountains being more mixed. By contrast, there is no similar pattern for pairs on non-capital cities, but rather the opposite.

We also examine pairs of all types of cities (capitals and non-capitals) and find that, conditional on the geodesic distance between them, they are more likely to belong to different states when the geography between them is more separating, as measured by the same three types of geography.

To illustrate this last result, we also construct maps showing Great Power territories as predicted by geography and the location of their capitals. The maps show striking resemblance to the actual state territories, with some interesting exceptions.

As a final note, not all capitals and state territories in Europe are the same today as they were centuries ago, but most arguably have deep historical roots. In that sense, we believe our study is relevant for understanding the political geography of Europe to this day.

References

Alesina, A. and Spolaore, E. (2003). *The Size of Nations*. MIT Press, Cambridge, Massachusetts.

Allen, T. (2023). The topography of nations. *NBER Working Paper*, No. 31795.

Bakker, J. D., Maurer, S., Pischke, J. S., and Rauch, F. (2021). Of Mice and Merchants: Connectedness and the Location of Economic Activity in the Iron Age. *The Review of Economics and Statistics*, 103(4):652–665.

Barjamovic, G., Chaney, T., Coşar, K., and Hortaçsu, A. (2019). Trade, merchants, and the lost cities of the Bronze Age. *Quarterly Journal of Economics*, 134(3):1455–1503.

Bleakley, H. and Lin, J. (2012). Portage and path dependence. *Quarterly Journal of Economics*, 127(2):587–644.

Bosker, M. (2022). City origins. *Regional Science and Urban Economics*, 94(103677).

Bosker, M. and Buringh, E. (2017). City seeds: Geography and the origins of the European city system. *Journal of Urban Economics*, 98:139–157.

Bosker, M., Buringh, E., and van Zanden, J. L. (2013). From Baghdad to London: unraveling urban development in Europe, the Middle East, and North Africa, 800-1800. *Review of Economics and Statistics*, 95(4):1418–1437.

Bremer, S. A. (1992). Dangerous dyads: Conditions affecting the likelihood of interstate war. *Journal of Conflict Resolution*, 36(2):309–341.

Colella, F., Lalive, R., Sakalli, S. O., and Thoenig, M. (2023). acreg: Arbitrary correlation regression. *The Stata Journal*, 23(1):119–147.

Collins, J. M. (1998). *Military Geography: For Professionals and the Public*. National Defense University Press, Washington, DC.

Cook, J. C. (2024). Subnational persistence of state history: evidence from geolocalized civilizations. *Mimeo, Tulane University*.

Dal Bó, E., Hernández-Lagos, P., and Mazzuca, S. (2022). The paradox of civilization: Preinstitutional sources of security and prosperity. *American Political Science Review*, 116:213–230.

Delventhal, M. J. (2018). The globe as a network: Geography and the origins of the world income distribution. *Mimeo, Claremont McKenna College*.

Diamond, J. (1997). *Guns, Germs, and Steel: The Fates of Human Societies*. W.W. Norton & Company, New York.

Dickens, A. and Lagerlöf, N. P. (2023). The long-run agglomeration effects of early agriculture in Europe. *Economic Inquiry*, 61(3):629–651.

Dincecco, M., Fenske, J., Gupta, B., and Menon, A. (2024). Conflict and gender norms. *SSRN Electronic Journal*.

Dincecco, M., Fenske, J., and Menon, A. (2021). The Columbian exchange and conflict in Asia. *SSRN Electronic Journal*.

Dincecco, M., Fenske, J., Menon, A., Mukherjee, S., Bentzen, J., Biroli, P., Cassidy, T., Chaudhary, L., Chiovelli, G., Dhar, S., Dittmar, J., Franco Vivanco, E., Gupta, B., Hassan, M., Kala, N., Koyama, M., Lee, A., Persaud, A., Satia, P., and Zhukov, Y. (2022). Pre-colonial warfare and long-run development in India. *The Economic Journal*, 132(643):981–1010.

Dincecco, M. and Onorato, M. G. (2016). Military conflict and the rise of urban Europe. *Journal of Economic Growth*, 21(3):259–282.

Ellingsen, S. (2025). Long-distance trade and long-term persistence. *Mimeo, University of Br*.

Engels, D. W. (1978). *Alexander the Great and the Logistics of the Macedonian army*. University of California Press, Berkeley and Los Angeles, California.

Fernández-Villaverde, J., Koyama, M., Lin, Y., and Sng, T.-H. (2023). The fractured-land hypothesis. *Quarterly Journal of Economics*, 138(2):1173–1231.

Flückiger, M., Larch, M., Ludwig, M., and Pascali, L. (2024). The dawn of civilization: metal trade and the rise of hierarchy. *CEPR Discussion Paper No. 18767*.

Galor, O. and Özak, Ö. (2016). The agricultural origins of time preference. *American Economic Review*, 106(10):3064–3103.

Gancia, G., Ponzetto, G. A., and Ventura, J. (2022). Globalization and Political Structure. *Journal of the European Economic Association*, 20(3):1276–1310.

Gleditsch, N. P. and Singer, J. D. (1975). Distance and international war, 1816–1965. In *Proceedings of the International Peace Research Association (IPRA) Fifth General Conference*, pages 481–506. IPRA, Oslo.

Henderson, J. V., Squires, T., Storeygard, A., and Weil, D. (2018). The global distribution of economic activity: nature, history, and the role of trade. *Quarterly Journal of Economics*, 133(February):357–406.

Hoffman, P. T. (2015). *Why Did Europe Conquer the World?* Princeton University Press, Princeton.

Iyigun, M., Nunn, N., and Qian, N. (2017). The long-run effects of agricultural productivity on conflict, 1400-1900. *NBER Working Paper*.

Jia, R. (2014). Weather shocks, sweet potatoes and peasant revolts in historical China. *Economic Journal*, 124(575):92–118.

Jones, E. (2003). *The European Miracle Environments, Economies and Geopolitics in the History of Europe and Asia*. Cambridge University Press, Cambridge, 3rd edition.

Kitamura, S. (2021). World historical battles database. *Mimeo, Osaka University*.

Kitamura, S. and Lagerlöf, N.-P. (2020). Geography and state fragmentation. *Journal of the European Economic Association*, 18(4):1726–1769.

Ko, C. Y., Koyama, M., and Sng, T.-h. (2018). Unified China and divided Europe. *International Economic Review*, 59(1):285–327.

Kulka, A. and Smith, C. (2024). When is long-run agglomeration possible? evidence from county seat wars. *Mimeo, University of Warwick*.

Laouenan, M., Bhargava, P., Eyméoud, J. B., Gergaud, O., Plique, G., and Wasmer, E. (2022). A cross-verified database of notable people, 3500BC-2018AD. *Scientific Data*, 9(1):1–19.

Levy, J. S. (1983). *War in the Modern Great Power System, 1495-1975*. University Press of Kentucky, Lexington, Kentucky.

Lipinski, R. (2024). Historical kaleidoscope: frequency of border changes and the long-term political and economic development in Europe. *Mimeo, University of Oxford*.

Maloney, W. F. and Valencia Caicedo, F. (2016). The persistence of (subnational) fortune. *Economic Journal*, 126(598):2363–2401.

Michaels, G. and Rauch, F. (2018). Resetting the Urban Network: 117-2012. *Economic Journal*, 128(608):378–412.

Nagy, D. K. (2023). Hinterlands, city formation and growth: evidence from the U.S. westward expansion. *The Review of Economic Studies*, 90(6):3238–3281.

Nüssli, C. (2010). Euratlas georeferenced vector data description. *Mimeo, Euratlas-Nüssli, Concise, Switzerland*.

Pounds, N. J. (1972). *Political Geography*. McGraw-Hill, New York.

Rappaport, J. and Sachs, J. D. (2003). The United States as a coastal nation. *Journal of Economic Growth*, 8(1):5–46.

Rohner, D., Thoenig, M., and Zilibotti, F. (2013). War signals: A theory of trade, trust, and conflict. *Review of Economic Studies*, 80(3):1114–1147.

Scheidel, W. (2019). *Escape from Rome: The Failure of Empire and the Road to Prosperity*. Princeton University Press, Princeton.

Schönholzer, D. and Weese, E. (2022). Creative destruction in the European state system: 1000-1850. *Mimeo, University of California Santa Cruz, and ISS, Tokyo University*.

Spate, O. H. K. (1942). Factors in the development of capital cities. *Geographical Review*, 32(4):622–631.

Spolaore, E. (2023). The Economic Approach to Political Borders. In Wilson, T. M., editor, *Border Studies: A Multidisciplinary Approach*. Edward Elgar Publishing, Cheltenham and Northampton.

Spolaore, E. and Wacziarg, R. (2006). The Diffusion of Development. *NBER Working Paper*, 12153.

Spolaore, E. and Wacziarg, R. (2009). The Diffusion of Development. *The Quarterly Journal of Economics*, 124(2):469–529.

Spolaore, E. and Wacziarg, R. (2016). War and relatedness. *Review of Economics and Statistics*, 98(5):925–939.

Toynbee, A. (1970). *Cities on the Move*. Oxford University Press, New York and London.

Treivish, A. I. (2016). Capital cities and state borders: spatial relationships and shifts. *Regional Research of Russia*, 6(3):244–257.

Weese, E. (2023). European political boundaries as the outcome of a self-organizing process. *Jounal of Social Science*, 74:21–43.

Tables and Figures

	Dependent variable is the Battle Indicator						
	(1)	(2)	(3)	(4)	(5)	(6)	(7)
Shortest-Distance Corridor Indicator	0.171***	0.170***	0.176***	0.146***	0.079***	0.069**	0.146**
	(0.019)	(0.019)	(0.019)	(0.017)	(0.020)	(0.032)	(0.049)
Sea Indicator		−0.011***	−0.011***		−0.039**		
		(0.003)	(0.003)		(0.019)		
Mountain Indicator (800 m)		−0.006	−0.006		−0.026		
		(0.005)	(0.004)		(0.036)		
Marsh Indicator		−0.018***	−0.018***		−0.007		
		(0.004)	(0.004)		(0.032)		
R^2	0.03	0.03	0.05	0.21	0.19	0.61	0.21
Number of obs.	15950	15950	15950	15950	1379	1379	15950
Fixed effects	None	None	GP-pair	GP-pair, Cell	GP-pair	GP-pair, Cell	GP-pair, Cell
Sample	Full	Full	Full	Full	Cells < 300 km of SD Corr.	Cells < 300 km of SD Corr.	Full
Standard errors	Robust	Robust	Robust	Robust	Robust	Robust	Clustered

Notes: Ordinary least squares regressions. Robust standard errors are indicated in parentheses, except for column (7), which uses two-way clustering on pairs and cells. The unit of observation is a cell/Great-Power pair combination. The Shortest-Distance (SD) Corridor is an indicator variable for whether a cell is intersected by a 50 km buffer zone around the Shortest-Distance line between the relevant pair of capitals. Columns (5) and (6) restrict the sample to cells intersected by a 300 km buffer zone around the shortest-distance line between capitals. * indicates p <0.10, ** p <0.05, and *** p <0.01.

Table 1: Battle locations and the shortest-distance corridor.

	Dependent variable is the Battle Indicator						
	(1)	(2)	(3)	(4)	(5)	(6)	(7)
Shortest-Distance Corridor Indicator	0.243***	0.181***	0.176***	0.286***	0.288***	0.248***	0.248***
	(0.031)	(0.021)	(0.020)	(0.037)	(0.036)	(0.034)	(0.071)
Sea Indicator	−0.004*			−0.006**	−0.006**		
	(0.002)			(0.003)	(0.003)		
Mountain Indicator (800 m)		0.002		−0.001	−0.002		
		(0.004)		(0.004)	(0.004)		
Marsh Indicator			−0.010***	−0.013***	−0.014***		
			(0.003)	(0.004)	(0.004)		
Sea × SD-Corridor	−0.137***			−0.168***	−0.162***	−0.141***	−0.141**
	(0.038)			(0.041)	(0.040)	(0.037)	(0.060)
Mountain × SD-Corridor		−0.103**		−0.171***	−0.166***	−0.177***	−0.177**
		(0.052)		(0.054)	(0.054)	(0.045)	(0.075)
Marsh × SD-Corridor			−0.066	−0.135**	−0.130**	−0.135**	−0.135
			(0.060)	(0.065)	(0.065)	(0.053)	(0.093)
R^2	0.04	0.03	0.03	0.04	0.05	0.22	0.22
Number of obs.	15950	15950	15950	15950	15950	15950	15950
Fixed effects	None	None	None	None	GP-pair	GP-pair, Cell	GP-pair, Cell
Standard errors	Robust	Robust	Robust	Robust	Robust	Robust	Clustered

Notes: Ordinary least squares regressions. Robust standard errors are indicated in parentheses, except for column (7), which uses two-way clustering on pairs and cells. The unit of observation is a Cell/Great-Power pair combination. The Shortest-Distance (SD) Corridor is an indicator variable for whether a cell is intersected by a 50 km buffer zone around the shortest-distance line between the relevant pair of capitals. * indicates p <0.10, ** p <0.05, and *** p <0.01.

Table 2: Battle locations and the shortest-distance corridor: interactions with geography.

	Dependent variable is the Geodesic Distance Between Capitals							
	(1)	(2)	(3)	(4)	(5)	(6)	(7)	(8)
Fraction Sea	-1.267^{***}			-1.348^{***}	-1.462^{***}		-1.348^{***}	
	(0.208)			(0.203)	(0.211)		(0.217)	
Fraction Mountain		1.209^{***}		0.577^{**}	0.116		0.577	
		(0.254)		(0.285)	(0.316)		(0.372)	
Fraction Marsh			-20.745^{***}	-27.307^{***}	-27.633^{***}		-27.307^{***}	
			(4.678)	(4.975)	(4.938)		(5.670)	
Separatedness Index						-4.973^{***}		-4.973^{***}
						(1.373)		(1.590)
R^2	0.56	0.51	0.51	0.61	0.60	0.52	0.61	0.52
Number of obs.	435	435	435	435	419	435	435	435
Sample	Full	Full	Full	Full	Dropping pairs in same country in 1900 or today	Full	Full	Full
Standard errors	Robust	Robust	Robust	Robust	Robust	Robust	Clustered	Clustered

Notes: Ordinary least squares regressions across city pairs made up by those cities which were capitals in 1800 according to Bosker et al. (2013), plus St Petersburg. Robust standard errors are indicated in parentheses, except for columns (7) and (8), which are identical to those in columns (4) and (6), respectively, but cluster standard errors on cell pairs. The dependent variable is the geodesic distance between the capitals, i.e., the length of the corridor. Column (6) drops those pairs of capitals where both are located within the same country in either 1900 (according to Euratlas), or today (as defined by GADM); all those pairs include a city in Italy or Germany. All specifications include city fixed effects. * indicates $p < 0.10$, ** $p < 0.05$, and *** $p < 0.01$.

Table 3: The effects of geography on the geodesic distance between capitals.

	Dependent variable is the Same-State Indicator in 1900						
	(1)	(2)	(3)	(4)	(5)	(6)	(7)
Length of Corridor	−0.291***	−0.292***	−0.294***	−0.283***	−0.283***	−0.283***	−0.283***
	(0.001)	(0.001)	(0.001)	(0.001)	(0.001)	(0.018)	(0.018)
Fra Sea along Corr.	−0.352***			−0.532***		−0.532***	
	(0.003)			(0.004)		(0.047)	
Fra Mountain along Corr.		−0.207***		−0.669***		−0.669***	
		(0.007)		(0.008)		(0.133)	
Fra Marsh along Corr.			1.132***	−4.270***		−4.270*	
			(0.361)	(0.392)		(2.317)	
Separatedness Index					−3.289***		−3.289***
					(0.022)		(0.302)
R^2	0.30	0.27	0.27	0.33	0.33	0.33	0.33
Number of obs.	241860	241860	241860	241860	241860	241860	241860
Standard errors	Robust	Robust	Robust	Robust	Robust	Clustered	Clustered

Notes: Ordinary least squares regressions across city pairs made up by cities which has a population above 5,000 in 1800, plus St Petersburg. Robust standard errors are indicated in parentheses, except for columns (6) and (7), which cluster on cell pairs. The dependent variable is an indicator taking the value one if the two cities belonged to the same state in 1900, and zero otherwise. All specifications include city fixed effects. * indicates p <0.10, ** p <0.05, and *** p <0.01.

Table 4: Same state outcomes across city pairs.

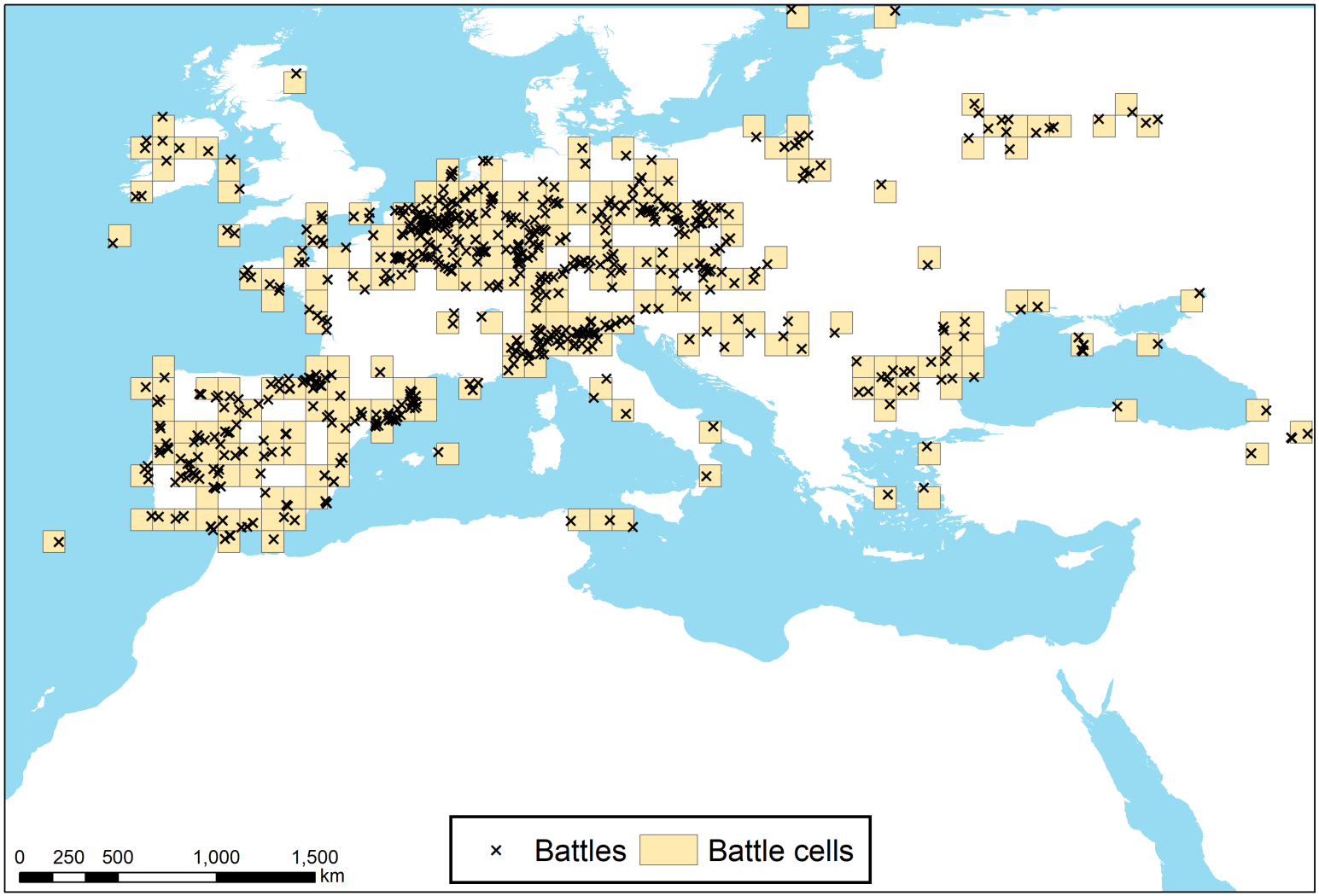

Figure 1: Map of all battles and battle cells.

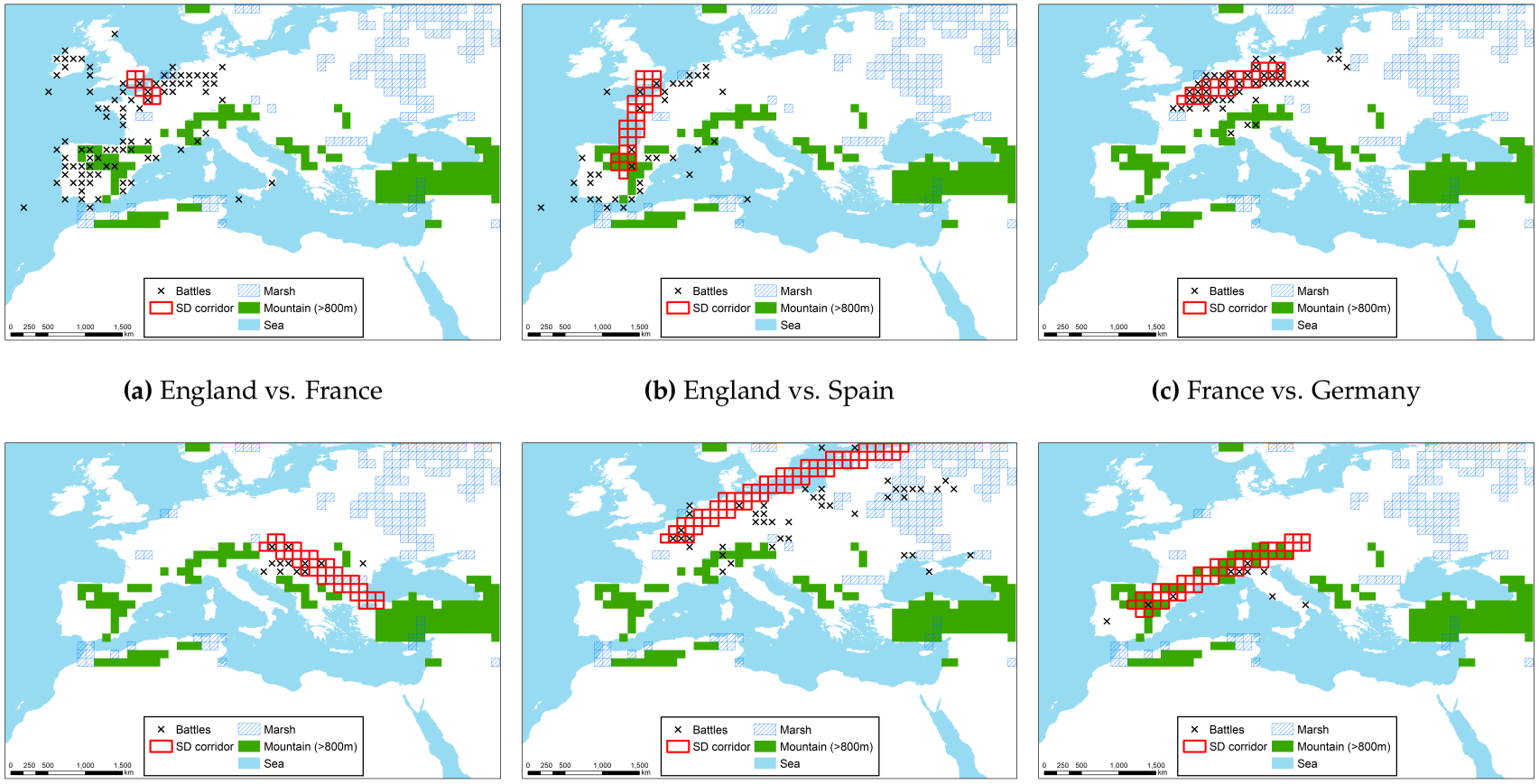

(a) England vs. France **(b)** England vs. Spain **(c)** France vs. Germany

(d) Ottoman Empire vs. Austria **(e)** France vs. Russia **(f)** Austria vs. Spain

Figure 2: Maps of some Great Power battles.

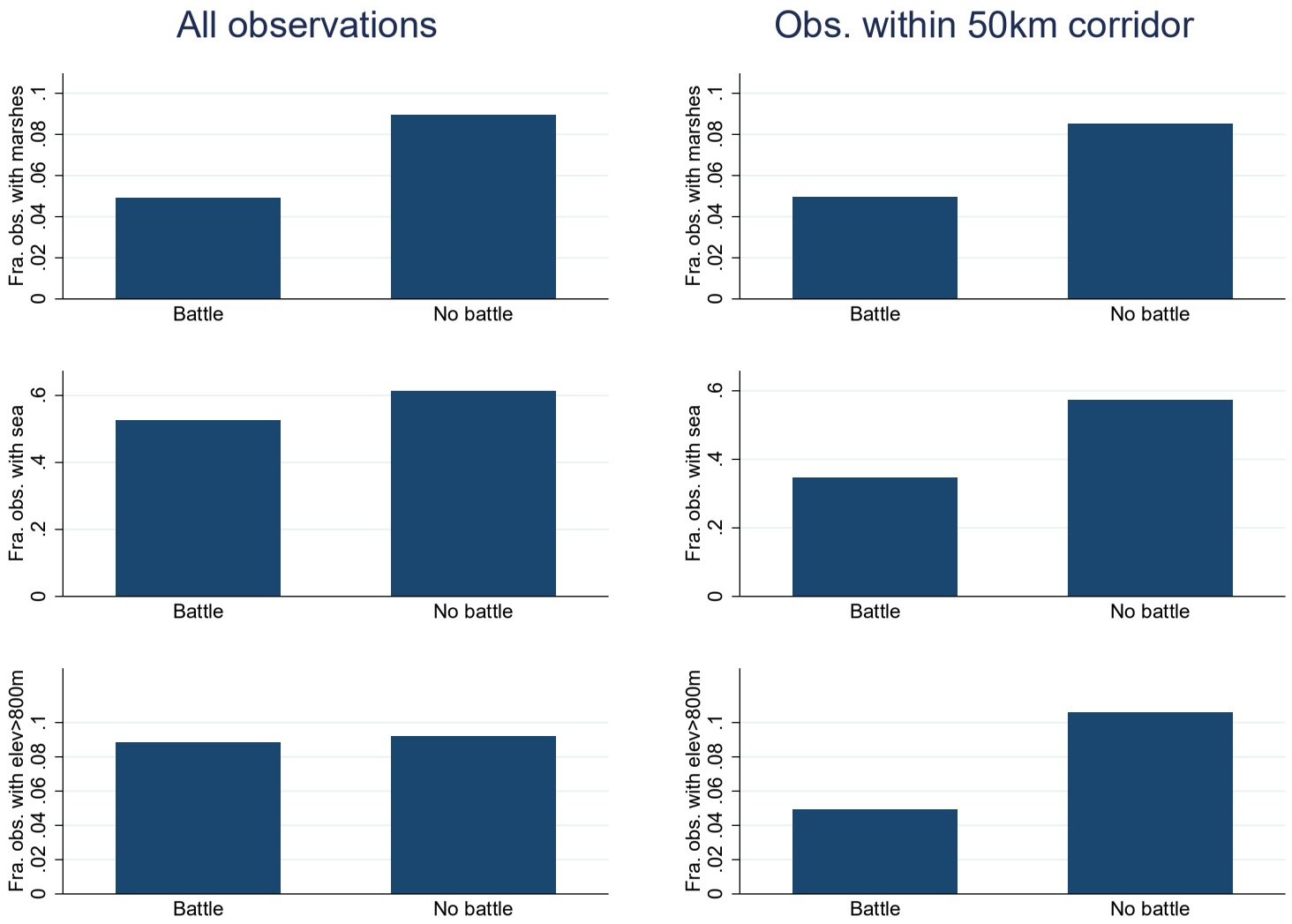

Figure 3: How geography differs between cell-pairs with and without battles, for the full sample and for cell-pairs close to the shortest-distance corridor between the belligerents' capitals.

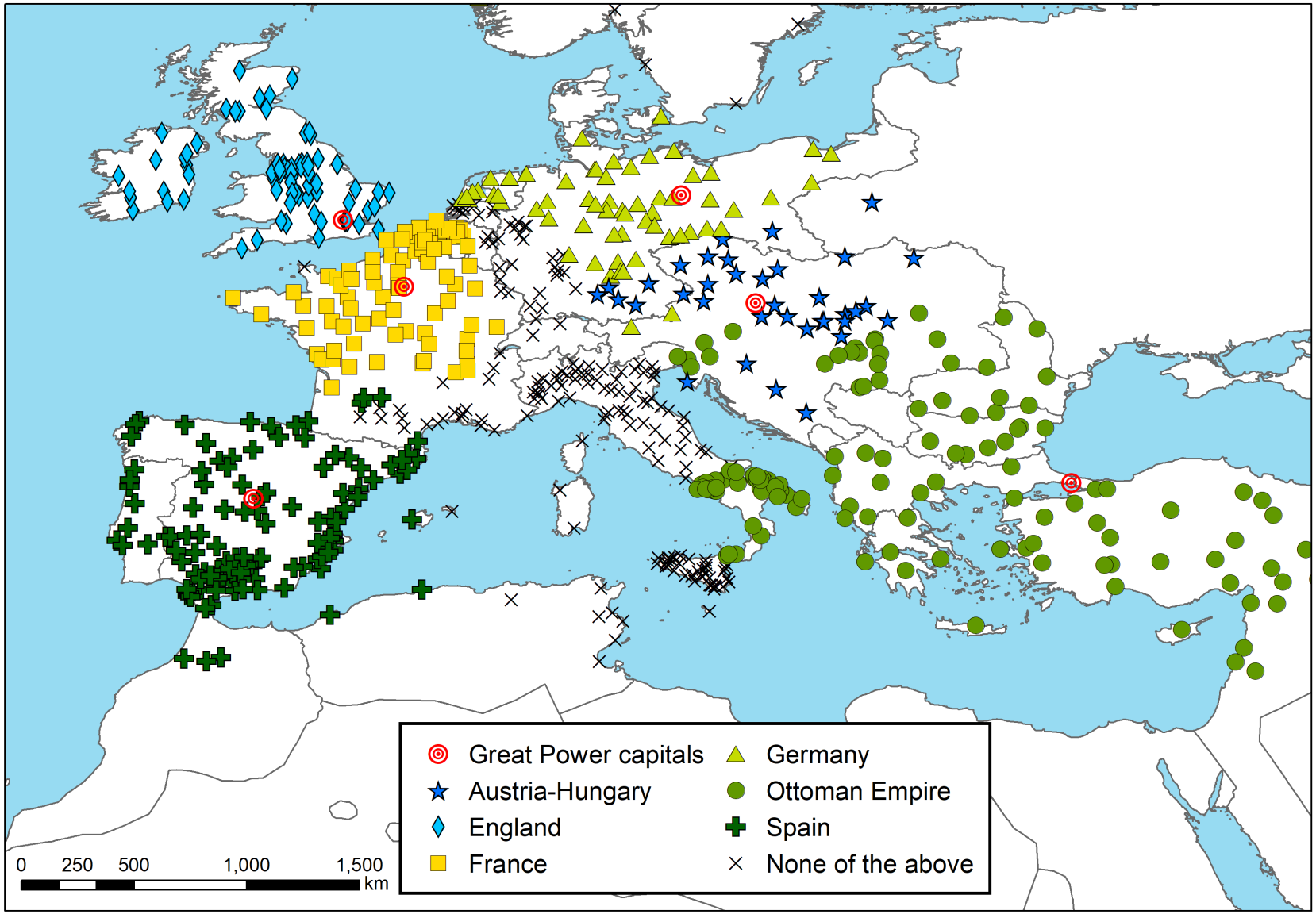

Figure 4: Predicted Great Power territories, interpreted as the Great Powers that cities are most likely to belong to given the location of the Great Power capitals (red circles). We assume that cities belong to no Great Power if the highest predicted probability falls below 0.15.

A Online Appendix

A.1 A Model

This section proposes a very simple spatial model to help interpret some of our empirical results. Locations are represented by points on a unit-length circle and indexed by $x \in [0, 1]$. To facilitate graphical illustrations, we project that circle to the unit interval, letting locations 0 and 1 be the same (i.e., where the circle closes).

We let "separatedness"at location x be denoted by a differentiable function $g(x)$. Empirically, a high $g(x)$ would correspond to more mountains, sea, and/or marshland at x.

There are N states indexed by $i \in \{1, 2, ..., N\}$. State i has a capital at location λ_i. (Each state also has one non-capital city; see below.)

Since the space is circular, the neighbor to the left of state 1 is state N, and, vice versa, the neighbor to the right of state N is state 1.

We distinguish between geodesic and effective distances. More precisely, consider two states, i and $i-1$, where $\lambda_i - \lambda_{i-1}$ represents the geodesic distance between their capitals. We let $E_{i-1,i}$ denote the corresponding effective distance, given by

$$E_{i-1,i} = \int_{\lambda_{i-1}}^{\lambda_i} g(x)dx = G(\lambda_i) - G(\lambda_{i-1}), \tag{A.1}$$

where $G(x) = \int_0^x g(z)dz$ and $G'(x) = g(x)$.

In other words, for a given geodesic distance between two capitals the effective distance is greater when the geography between them, as measured by the levels of $g(x)$, is more separating. Figure A.1 provides an illustration.

The next section describes how states optimally locate their capitals, which is the only decision made in this model, and the resulting equilibrium. Once we have determined the equilibrium distribution of capitals, borders between states are assumed to be located geodesically halfway between capitals, thus defining state territories; see Section A.1.3 below.

Each state's (single) non-capital city is then assumed to be located at the point within its territory that has the lowest separatedness. This is not modelled as a choice but motivated with some further discussion in Section A.1.4 below.

A.1.1 The Location of Capitals

Each state is assumed to locate its capital to maximize the product of the effective distances to its neighboring capitals. Although we do not model conflict explicitly, the idea is that states want to keep capitals secure from attacks by hostile neighbors. We write the objective function for state i as:

$$\pi_i = E_{i-1,i} \times E_{i,i+1}. \tag{A.2}$$

Because this is a coordination game, where each capital's optimal location depends on where its neighbors' capitals are located, there are multiple equilibria. To select one equilibrium, we need to arbitrarily fix the location for one of the capitals. Here we let state N's capital be located at point 1, which (recall) is the same as point 0. This will later be verified to be optimal for state N in equilibrium.

Consider now a state $i \in \{2, ..., N-1\}$, which sets λ_i to maximize (A.2), subject to (A.1), and (A.1) forwarded to $E_{i,i+1} = G(\lambda_{i+1}) - G(\lambda_i)$, taking as given the locations of the neighboring states' capitals, λ_{i-1} and λ_{i+1}.

The first-order condition can be seen to imply that the effective distances are equalized: $E_{i-1,i} = E_{i,i+1}$.[12] Using (A.1), this can be written

$$G(\lambda_i) - G(\lambda_{i-1}) = G(\lambda_{i+1}) - G(\lambda_i). \tag{A.3}$$

This hints at the main mechanism in this model: where $g(x)$ is high, and $G(x)$ steep, the geodesic distance between capitals is shorter, since a given distance between λ_i and λ_{i-1} is associated with a greater gap between $G(\lambda_i)$ and $G(\lambda_{i-1})$. That is, a more separating geography affords a shorter geodesic distance between capitals.

Note also that the effective distance between state 1 and state N (and vice versa) equals $G(\lambda_1)$: state 1's leftward neighbor is state N with its capital at location 0 (same as location 1), and $G(0) = 0$. Likewise, the optimality condition for state 1—corresponding to that in (A.3)—becomes $G(\lambda_1) = G(\lambda_2) - G(\lambda_1)$.

[12] The first-order condition can be written $G'(\lambda_i)/E_{i-1,i} = G'(\lambda_i)/E_{i,i+1}$, which simplifies to $E_{i-1,i} = E_{i,i+1}$.

A.1.2 Equilibrium

As mentioned, the capital of the Nth state is set where the circle closes: at location 1, which (recall) is the same location as 0. We can now state the following.

Proposition 1. *Assume that $\lambda_N = 1$. Then the equilibrium location for the capital of state i is defined from*

$$G(\lambda_i) = \frac{iG(1)}{N}. \tag{A.4}$$

Proof. Define the effective distance between the capital of state i and the capital of its neighbor to the left as

$$\chi_i = G(\lambda_i) - G(\lambda_{i-1}), \tag{A.5}$$

with $\chi_1 = G(\lambda_1)$, since (recall) state 1's neighbor to the left (state N) has its capital at 0 (same as 1). We know from (A.3) that χ_i equals the same constant for all states $i \in \{2, ..., N-1\}$. Call that constant $\overline{\chi}$.

For state 1, we also have $\chi_1 = G(\lambda_1) = \overline{\chi}$, since it equalizes the effective distance from its capital to both its neighbors' capitals, and the effective distance to its rightward neighbor's capital equals $G(\lambda_2) - G(\lambda_1) = \chi_2 = \overline{\chi}$.

The same holds for state N: the effective distances to the capitals of its neighbors to the right and left must equalize for its capital location to be chosen optimally, so χ_N must equal the effective distance between the capitals of states 1 and N, i.e., $\chi_N = \chi_1 = \overline{\chi}$.

Thus, $\chi_i = \overline{\chi}$ for all states $i \in \{1, ..., N\}$, implying that $\sum_{i=1}^{N} \chi_i = \overline{\chi}N = G(1)$ [recalling that $G(0) = \int_0^0 g(z)dz = 0$], which gives

$$\overline{\chi} = \frac{G(1)}{N}. \tag{A.6}$$

We now see that $G(\lambda_1) = \chi_1 = \overline{\chi} = G(1)/N$. Then (A.5) says that $G(\lambda_2) = G(1)/N + G(\lambda_1) = 2G(1)/N$; $G(\lambda_3) = 3G(1)/N$; and so on, with $G(\lambda_N) = NG(1)/N = G(1)$. This implies the solution in (A.4). ■

Intuitively, if the terrain is constant, meaning $g(x)$ is constant and $G(x)$ linear, the distances will be the same between any two capitals. That is, (A.4) shows that, when $G(\lambda_i)$ is linear, then $\lambda_i - \lambda_{i-1}$ becomes the same for all i. The reason geodesic distances

vary between different pairs of capitals in this model is because $g(x)$, and thus $G(x)$, vary across space.

Note also that, because the effective distances between all capitals equalize in equilibrium, $\lambda_N = 1$ is optimal for state N. That is, the effective distance between 0 and λ_1 is the same as that between λ_{N-1} and 1. State 1 also locates its capital optimally, since (A.4) satisfies $G(\lambda_1) = G(\lambda_2) - G(\lambda_1)$. Similarly for the remaining states $i \in \{2, ..., N-1\}$, the optimality condition in (A.3) is implied by (A.4).

One simple case that allows us to solve for λ_i analytically is when $g(x) = x$, and $G(x) = x^2/2$. Then we see that $G(\lambda_i) = \lambda_i^2/2 = iG(1)/N = i/(2N)$. Disregarding the negative root (for obvious reasons) it follows that

$$\lambda_i = \sqrt{\frac{i}{N}}. \tag{A.7}$$

A.1.3 Territories

To define state territories, we let borders be located at the geodesic halfway point between capital. That is, the left border of state i is halfway between λ_i and λ_{i-1} at $(\lambda_i + \lambda_{i-1})/2$; the right border of the same state is located at $(\lambda_{i+1} + \lambda_i)/2$.

A.1.4 The Location of Non-Capital Cities

Given state territories, we assume that the single non-capital city of each state is located at the point within its territory that has the lowest separatedness, i.e., at the $x \in [\frac{\lambda_i+\lambda_{i-1}}{2}, \frac{\lambda_{i+1}+\lambda_i}{2}]$ where $g(x)$ is minimized. This could be at one of the borders, $\frac{\lambda_i+\lambda_{i-1}}{2}$ or $\frac{\lambda_{i+1}+\lambda_i}{2}$, or at an interior minimum point within that territory.

The broad idea we want to capture is that non-capital cities benefit from being well connected locally, implying low $g(x)$. Alternatively, we could assume that non-capital cities tend to emerge at locations with abundant natural resources and/or high agricultural productivity. If this means less separating geography (fewer seas, mountains, and marshes), then such features should be inversely related to $g(x)$.

The assumption of one non-capital city per state may be interpreted as each state constituting a free-trade area with a single trade hub. This assumption is not necessary for

the model to generate the results we are after, but rather works against us, since it implies more non-capital cities where there are more states, and thus where $g(x)$ is high. If larger territorial states had more non-capital cities than smaller ones, then we would see more of them where $g(x)$ is low.

A.1.5 Simulations

Functional Forms

With an assumption about N and a functional form for $g(x)$ we can determine the equilibrium location of each capital on the circle. Together all capital locations then define territories and non-capital city locations.

For some parametric cases we can easily find analytical solutions, as when $g(x) = x$ mentioned just above; see (A.7). With richer functional forms for $g(x)$ it is easiest to use numerical illustrations.

Figure A.2 considers the example where $g(x) = x^2(1-x)^2(x-1/4)^2(x-2/3)^2$ and $N = 10$. Panel A plots $g(x)$ against x and shows three other items on the horizontal (x) axis: (i) the equilibrium locations of the capitals; (ii) the resulting territorial borders located geodesically halfway between capitals; and (iii) the location of each state's single non-capital city at the point where $g(x)$ is minimized within its territory.

In Panel B we consider all different pairs of capitals, which comes to $N(N-1)/2 = 45$ pairs in this case, with $N = 10$. Across these 45 pairs, we plot the geodesic distance between the capitals in each pair (as measured on the circle and thus between 0 and $1/2$) against the average level of separatedness, $g(x)$, between them (here normalized to fall between 0 and 1). While it is not obvious to see with only 45 observations, the relationship in Panel B of Figure A.2 is negative with a correlation coefficient of $-.62$.

In Panel C we do the same thing as in Panel B, but for non-capital cities. Here the correlation coefficient comes out as $-.12$, which is closer to zero than in Panel B. The correlations in Panels B and C of Figure A.2 refer to one functional for $g(x)$ and one assumption about N, but as we shall see soon this tends to be a more systematic pattern.

Finally, we explore if a more separating geography also results in more state fragmen-

tation. In Panel D, we consider multiple pairs of locations (not only capitals or non-capital cities), all at the same fixed distance, here set to 0.1, i.e., $1/10$ of the unit circle. The two bar graphs show how average separatedness between the two locations in each pair differs between those pairs which are located in the same state and those which are split between different states (i.e., located on different sides of a border, possibly more than one border). As seen, separatedness tends to be lower for pairs of locations in the same state, compared to those in different states. While this may seem obvious from the fact that borders tend to cluster where $g(x)$ is high (see Panel A), note that this result holds when considering a fixed distance between the locations, which makes it comparable to our regression results, where we control for geodesic distances.

As noted, the results in Figure A.2 refer to one functional for $g(x)$ and one assumption about N. In a sense, it also hinges on our assumption that the capital of state N to be located ay point 1 (the same as point 0), but this is mirrored in the assumed shape of $g(x)$, which we can shift arbitrarily across the $[0, 1]$ space.

Figure A.3 explores a geography like that in Figure A.2, but inverted, meaning that the minimum points in A.2 become maximum points in Figure A.3, and vice versa. In other words, we multiply by minus one and add a constant to make $g(x) \geq 0$ for all $x \in [0, 1]$. Like before, we assume that the capital of state 1 is located at $x = 0$ (and $x = 1$), which is here a (local) maximum point, and still consider $N = 10$ states. The patterns across all panels is qualitatively the same as in Figure A.2. Most importantly, the correlation coefficients in Panel B and C are here $-.44$ and .14, respectively. That is, the correlation for capital pairs is negative while that for non-capital city pairs is larger, here even positive.

Random Geographies

As mentioned, the functional forms used for $g(x)$ in Figures A.2 and A.3 are arbitrary. How consistent are the differences in correlations between separatedness and geodesic distance for pairs of capitals compared to pairs of non-capitals? To obtain a more complete picture, we next consider randomly generated geographies, meaning that $g(x)$ is produced through a random walk. We let $g(0) = 0$ and then generate values for $g(x)$ at

discrete intervals using $g(x + .001) = g(x) + .01r(x)$, where $r(x)$ is a random draw from a standard normal distribution with zero mean and standard deviation of one. We then add a constant so that it $g(x) \geq 0$ holds everywhere. The outcome for one such random geography is shown in Figure A.4. Like with the examples in Figures A.2 and A.3, we can visually assess that the correlations are negative for capitals in Panel B and more positive or zero for non-capitals in Panel C.

We can then do a Monte Carlo simulation, where we repeat the same exercise 5,000 times, saving the two correlation coefficients of interest for each randomized geography. The upshot is two overlapping histograms for the correlation coefficients: one referring to pairs of capitals and the other to pairs of non-capitals. These are shown in Figure A.5. The correlation across pairs of capitals is always negative, while those for non-capital cities can be positive or negative, with some mass above zero. This qualitatively matches the empirical results. More separatedness tends to be associated with a shorter geodesic distances between pairs of capitals, but there is no similar robust pattern for pairs of non-capitals.

A.1.6 Possible Extensions

We could make the model much more realistic by allowing for, e.g., state heterogeneity, or an endogenous number of states. However, this need not affect any of the specific mechanisms that we are after here. For example, if we let states care about their territorial size, that would not change anything. With borders located geodesically half-way between capitals, the territory of state i becomes $(\lambda_{i-1} + \lambda_{i+1})/2$, which does not depend on λ_i.

A.2 Battle Data Analysis: Robustness and Further Exploration

A.2.1 Summary Statistics

Table A.1 presents summary statistics for some of the variables used in the battle data analysis. For the battle and SD corridor indicators, we show the statistics for the full set of cell and GP pairs. For the geography variables, we consider only cells, since these do not vary across GP pairs. For comparison, we also show the same statistics for land cells.

Some of the geography variables not used in the benchmark analysis are discussed in Section A.2.3 below.

A.2.2 Alternative Corridors

The benchmark analysis considers corridors between Great Power capitals. Here we examine how the results change with completely different corridors. We consider two alternatives: (1) corridors around the territorial borders, or contours, of the Great Powers involved, what we call *contour corridors*; and (2) corridors around shortest-distance lines that connect the largest non-capital cities, which we label *non-capital corridors*. In both cases, we let the corridors be 50 km wide, as we did for our benchmark measure. These variables take the value one for cells intersected by the alternative corridor associated with each respective Great Power pair, and zero otherwise. See maps in Figures A.6 and A.7.

Contour Corridors

The contour corridors are based on maps for 1900 from Euratlas (Nüssli, 2010). We choose the year 1900 in part because Europe had the smallest number of states around then, and on average the territorially largest Great Powers. We also want borders to be a meaningful measure of the territorial reach of state capacity, which may have been more limited in earlier centuries. We here only consider contours around the core segments of the respective states, ignoring colonies and overseas dominions. For example, we ignore Britain's holdings in Egypt. Note also from Figure A.6 that these corridors can cover almost the whole country (see, e.g., Great Britain).

Non-Capital Corridors

We want the non-capital corridors to run between the largest non-capital cities of each Great Power. Which cities to choose is not always obvious, since both city rankings and state borders can change over time, and how they change depends on which time period we consider.

To fix ideas, we focus on the period from 1800, the last year for which Bosker et al. (2013) has city population data, up until today. Given this time period, the choice of city is relatively straightforward in most cases. Great Britain's largest city after London was Manchester in 1800, according to Bosker et al. (2013), and it remains second largest in the United Kingdom today, according to Wikipedia. Using similar criteria, we choose Izmir (or Smyrna) for the Ottoman Empire (Ankara was much smaller up until it became the capital of Turkey) and Hamburg for Germany.

In the case of France, we choose Marseille, which was slightly smaller than Lyon in 1800, but is the second largest city after Paris today.

For Austria-Hungary, we choose Budapest. Bosker et al. (2013) report population data for the two cities Buda and Pest separately, with a total population of 50,000 in 1800. Graz and Debrecen (or Debreczin) are the closest runner-ups among cities located in today's Austria or Hungary; neither had a population exceeding that of Budapest in 1800 or today, according to Bosker et al. (2013) and Wikipedia, respectively.

For Spain, we choose Barcelona, which was the largest city in Spain in 1800 according to Bosker et al. (2013), at least if we exclude the capital Madrid. Although not part of Spain through much of its existence, Barcelona was absorbed into Spain in 1714 with the fall of the independent Principality of Catalonia.

For Russia, we do not have any population data from Bosker et al. (2013), but given that our benchmark analysis uses St Petersburg as capital, it makes sense to choose Moscow as our largest non-capital city. This is the current capital and also largest city of Russia.

Results With Alternative Corridors

Table A.2 shows, for each Great Power, the correlation between our benchmark measure (i.e., the shortest-distance corridor between capitals), and our two alternative corridor indicators. For some pairs, the correlations are relatively large, meaning the corridors overlap a great deal. This is the case for, e.g., Austria-Germany, where the alternative Hamburg-Budapest corridor has a correlation coefficient of .57 with the benchmark Berlin-Vienna corridor. For other Great Power pairs, the capital/non-capital corridor correlations are much smaller or even negative. By comparison, the contour corridors show

low but positive correlations with the benchmark capital corridors, and these are relatively stable across Great Power pairs.

Table A.3 presents results from the same regressions as in Table 1 when adding the contour corridor indicator as control. Table A.4 instead adds the non-capital corridor as control and Table A.5 adds both. In all these regressions, the alternative corridor measures come out as positive and significant, which is perhaps not too surprising, since both tend to be positively correlated with our benchmark measure (cf. Table A.2). More importantly, the coefficients on our benchmark corridor measure stays positive and significant and comes out as larger and more significant than the other two. This holds in all specifications. There is little to suggest that our main findings are due to battles tending to be fought in adjacent or overlapping regions, such as the territorial peripheries of the Great Powers, rather than in the corridors between the actual capitals. In other words, our results do not appear to be spurious.

The results in columns (5)-(6) in Table A.4 are particularly interesting, just like the corresponding columns in Table 1. These columns restrict the samples to cells located within 300 km from the shortest-distance lines between capitals. In these specifications, the alternative measures come out as (mostly) insignificant and smaller than the benchmark corridor. That is, the difference in results is particularly noticeable locally around the corridors between capitals.

Of course, this 300 km sample restriction is itself based on the benchmark corridor measure. Table A.6 examines alternative sample restrictions as well. Column (1) first presents results when regressing the battle indicator on the benchmark corridor with both cell and GP pair fixed effects and using the full sample. Column (2) then restricts the sample to cells within 300 km of the benchmark corridors. The benchmark corridor comes out as significant in both specifications. This repeats what we already saw in Table 1.

Next, columns (3) and (4) of Table A.6 do the same for the non-capital corridor. Note that the sample restriction in column (4) is now based on cells within 300 km of the *non-capital* corridor. We obtain a positive coefficient on the non-capital corridor in column (4), but it is smaller and less significant than that for the capital corridor in column (2). In columns (5) and (6) we add the benchmark corridor measure as control to the same

specifications as in (3) and (4). That is, we let the sample restriction in column (6) be cells within 300 km of the non-capital corridor. We again see the benchmark measure doing marginally better. Finally, column (7) restricts the sample to cells within 300 km of *both* corridors. This shrinks the sample to just 792 observations, and with cell and GP pair fixed effects we do not get any significant estimates, but it is worth noting that the point estimate on the benchmark corridor is positive, while that on the non-capital corridor is negative. In sum, the results that we found locally around the benchmark capital corridors are not specific to that particular sample restriction. Regardless of how we choose the specifications and sample restrictions, the benchmark measure tends to always perform better.

A.2.3 Alternative Geography Measures

The main analysis considered three types of geography—seas, mountains, and marshland—all of which we argued should have hindered military transport. Here we consider three other geography variables, namely indicators for the presence of rivers and lakes, and high levels of the Caloric Suitability Index (CSI). The last one of these is from Galor and Özak (2016), with our indicator taking the value one for cells in the 90th percentile of CSI across all cells in our dataset. Data on lakes and rivers are from Natural Earth (`www.natural-earthdata.com`). We here use indicators for any lake or river entering the cell. Some descriptive statistics are presented in Table A.1; note that almost 40% of all cells, and about 70% of all land cells, are intersected by a river.

In Table A.7 we present results from a few regressions where we interact geography with the SD-corridor, similar to those in Table 2, but here including our three alternative geography measures as well as the three benchmark ones, both separately and together. Of the three alternative measures, the only significant results refer to the river indicator, which comes out as positive and significant. That is, rivers do not push battles off the shortest-distance corridor, but rather the opposite. The results for our benchmark measures do not change much, although the sea indicator comes out as insignificant in column (8), where we cluster standard errors. This may have to do with the majority of land cells having rivers, making that variable pick up some of the variation otherwise captured by

the sea indicator. As discussed in the main text, the existing literature suggest that the effect of rivers can be ambiguous.

A.2.4 Other Robustness Checks

Tables A.8 to A.16 explore further variations on the regressions in Table 2, meant to address some remaining concerns.

In the main analysis we defined cells with mean elevation above 800 meters as mountain cells. Table A.8 considers alternative definitions, using the same specifications as in column (6) of Table 2. The largest positive, and most significant, coefficients are found when using the 800-meter threshold. For very low levels of elevation the coefficients turn negative, which is due to cells at low elevation often having marshes, or being (fully or partially) covered by sea.

Table A.9 considers the same specifications as in Table 2, but uses only land battles when defining which cells are battle cells, dropping naval battles. This renders the negative interaction effect from sea cells more significant, for reasons that are rather obvious and not interesting. More importantly, the negative interaction effects for mountains and marshes stay robust.

The negative effect of the SD-distance corridor, and its interactions with geography, could be driven by battles happening close to the capitals between which the corridor spans. To explore this possibility, Table A.10 drops those cells that are closer than 200 km from any of the relevant capitals for each pair. The results are largely robust to this chance, with negative interaction effects throughout, slightly less significant for sea interactions and more significant for marshes, when compared to Table 2.

Not every military incursion was directly aimed at capturing the opponent's capital. The perhaps most well-known example is the French invasion of Russia in 1812. Even though the Russian capital was St Petersburg at the time, Napoleon actually advanced towards Moscow. Table A.11 presents regressions results similar to those in Table 2, keeping the battle indicator unchanged but assigning Moscow as the Russian capital instead of St Petersburg when constructing the corridor variable. The results change very little compared to those in Table 2.

In the benchmark analysis we disregarded Great Power pairs that fought fewer than 10 battles. We can instead consider the full set of 21 pairs, including those which fought no battles at all, which expands the dataset to 30,450 observations (i.e., 1450 cells and 21 pairs). For pairs involving Prussia/Germany or Russia, we let Berlin and St Petersburg be capitals. Table A.12 shows the results. Except for the coefficient on the interaction between the SD corridor and the marshland indicator becoming slightly less precisely estimated, the results are otherwise similar to those in Table 2.

Table A.13 presents the same regressions as in Table 2 but lets the dependent variable be the number of battles in the cell (between the relevant pair and from 1525 to 1913), rather than just a battle indicator. The results are robust to this change, and in fact strengthen for marshes in column (7).

Table A.14 allows for spatially adjusted standard errors and declining weights, applying the acreg command in Stata and the Bartlett option from Colella et al. (2023). The specifications are the same as in column (6) of Table 2, changing the distance cut-off within which standard errors are allowed to be correlated. The results are broadly consistent with the benchmark results, with slightly weaker results for marsh interactions, similar to when using two-way clustering in column (7) of Table 2.

One concern is that geography simply captures an effect of urbanization. For example, battles might not happen where the SD-corridor intersects mountains or marshes because those areas are uninhabited, which can make it hard to feed and service troops. To explore this, Table A.15 adds an interaction with cities along the SD-corridor to the specification in column (6) of Table 2. The variable we call City (or City Indicator) is equal to one for cells having a city with population above 5,000 in the year indicated for each column of Table A.15. Population data come from Bosker et al. (2013). For all years, there is a positive interaction effect between city presence and the corridor, meaning battles are more likely to happen on the SD-corridor where cities are located, i.e., in more populated areas. More importantly, the interaction effects with our three geography variables are robust to the inclusion of these city interactions.

The benchmark analysis focused on battles fought between 1525 and 1913. Table A.16 instead considers the period 1914-1945, i.e., the two world wars. We otherwise

follow the same steps as when we constructed the benchmark dataset, dropping pairs that fought fewer than ten battles and cells to the north/south/west/east of the more northerly/southerly/westerly/easterly battles. We then end up with 1470 cells instead of 1450, and 6 pairs instead of 11, and thus 8,820 observations rather than 15,950. We also let the corridor variable be based on Moscow rather than St Petersburg, since Moscow was the capital for most of the period considered. The results in Table A.16 show that the interaction effects for seas and marshes come out as insignificant, while the coefficients for mountains are mostly significant but somewhat smaller in size compared to Table 2. Although this could be due to the smaller sample, we also ran regressions on a larger dataset where we did not drop pairs that fought fewer than ten battles, resulting in 31,899 observations (1519 cells and 21 pairs). To conserve space we do not show those results here, but they come out as even weaker, with no significant interaction effects at all, even for mountains. Our conjecture is that these differences in results rather reflect how advances in military and transport technology from the early 20th century started to make geography less of an obstacle for advancing armies.

A.3 Geodesic Distances: Robustness and Further Exploration

A.3.1 Summary Statistics

Table A.17 presents summary statistics for the main variables used in the city level analysis, considering pairs of capitals and non-capitals separately. Note that some pairs have 100% mountain (elevation above 800 meters) between them, mostly referring to cities in today's Turkey, in particular Niğde and close neighbors. City pairs with almost only sea between them are located along the Mediterranean coast.

A.3.2 Non-Capitals

In Table A.18 we run the same regressions as in Table 3, but for pairs of cities where both are non-capitals according to Bosker et al. (2013), which comes to 221,445 unique pairs in total. As in Table 3, all specifications include city fixed effects.

The estimated coefficients on the fractions sea and mountain in columns (1) and (2)

come out positive and significant, while that for the fraction marshland is negative and significant in column (3), but turns insignificant when all three variables are entered together in column (4). The Separatedness Index also comes out as positive and significant in column (5).

In column (6) and (7) of Table A.18, where we cluster standard errors on cell pairs, the correlations become much less significant. Recall that we get significant negative estimates for capital pairs with the same cell-pair clustering; see columns (7) and (8) of Table 3. This strongly suggests that capitals are different from non-capitals. That is, a separating geography brings capitals closer, while there is no such effect for non-capitals, and if anything the opposite.

A.3.3 Size Differences for Capitals and Non-Capitals

Table A.19 analyses results for large cities, again looking at pairs of capitals and non-capitals separately. To conserve space, we consider the Separatedness Index as a single composite measure of geography.

Across the columns, we restrict the samples to pairs where both cities have populations above the 50th, 75th, 90th, and 95th percentiles, respectively. Population numbers are from Bosker et al. (2013) and refer to the year 1800. [Note that columns (1) and (3) are identical, because the set of capital city pairs is the same when restricting populations to be above median as when restricting them to be in the 75th percentile.]

Throughout in Table A.19, we find that the relationship between distances and separatedness is negative and mostly significant for pairs of capitals, while insignificant and carrying inconsistent sign for non-capitals. This shows that the patterns we describe for capitals is likely not caused by their size, but rather something else that makes them unique. Since large non-capital cities are likely to be commercial centers, these patterns seem broadly consistent with the idea that seperatedness matters more for security, and connectedness more for trade.

A.3.4 Alternative Definitions of Capitals

Our analysis so far has been based on capitals as defined by Bosker et al. (2013). There are of course different definitions of what constitutes a capital (and/or a sovereign state). It stands to reason that the mechanisms that we are after might easiest be found among states that are in regular conflict with each other, such as the Great Power nations of Europe.

Table A.20 shows some variations on the regression in column (6) of Table 3, again restricting attention to the Separatedness Index. Column (1) repeats the results found in Table 3, where we define capitals based on Bosker et al. (2013). Column (3) considers a smaller sample made up by the same Great Power capitals that we used in our battle analysis, what we call a narrow definition of Great Powers, while column (2) includes Stockholm and Amsterdam, which we call a broad definition. Because the samples in columns (2) and (3) are much smaller, the coefficients are less precisely estimated, but consistently negative. Figure A.9 shows the associated plots, where both the geodesic distance and the index are reported as residuals net of city fixed effects.

Columns (4)-(6) of Table A.20 consider the same regressions as in columns (1)-(3), but with standard errors clustered on cell pairs, with qualitatively similar results.

A.4 Same-State Outcomes: Robustness and Further Exploration

This section considers variations on the regressions in Table 4. Table A.21 presents results with the same-state indicator measured in 2000 based on Euratlas data (same source as in Table 4), and Table A.22 shows the results when using modern country borders from the Global Administrative Boundaries (GADM) database (version 3.6, the most recent at the time these data were extracted). The results when using these modern state borders are qualitatively very similar to those in Table 4, which were based on 1900 borders.

The location of cities with populations above 5,000 may well be endogenous to how state territories form. As yet another complementary exercise, Table A.23 thus considers similar gravity regressions as those in Table 4, but here across pairs formed only by cities present in 800 CE and in the year for which we measure same-state outcomes, which

we let vary from 800 CE to 1800 CE. Here all specifications include city fixed effects and standard errors are clustered on cell pairs.

While shrinking the sample considerably, dropping cities that emerged after 800 CE should mitigate some of these endogeneity concerns, since centralized statehood did not exist (or was at least not widespread) in Europe by then. The coefficient estimates in Table A.23 come out with roughly the expected negative signs: not all estimates are highly significant, but those that are carry the right (negative) sign.

Table A.24 presents results from the same regressions, but using the Separatedness Index instead of the three geography variables separately, which facilitates interpretation. The pattern is similar to Table A.23, with the most significant negative estimates around 1300-1500, and slightly less precise after 1600.

A.4.1 Comparing Predicted and Actual Territories Quanitatively

Table A.25 shows how well the size of the predicted territories, which (recall) are measured as the number of cities predicted to belong to the same Great Power as the capital, matches the corresponding actual territories in 1900, as defined by the Euratlas borders. As seen, the greatest mismatch is for the Ottoman Empire, which is predicted to cover 2.69 as many cities as it actually did cover in 1900. Spain's territory is also over-predicted, but the others match relatively well.

We can also explore how the predictions perform in terms of which cities are matched. To that end, we construct what we call an overlap ratio. This is defined as the ratio of the number of cities in *both* the predicted *and* actual territory of a Great Power over the number of cities in *either* its predicted *or* actual territory. The overlap ratio thus ranges from zero (no overlap) to one (perfect overap); see Figure A.13 for an illustration. As seen in Table A.25, this ratio is highest for England at .96 and lowest for Austria-Hungary at .46.

These numbers are calculated based on the actual capitals. We can instead let the cities that we used for the non-capital corridors (see Section A.2.2) serve as capitals when we predict the territories, while keeping the capitals of the other Great Powers fixed. Table A.25 shows that the overlap ratio becomes worse for all Great Powers, except Austria-

Hungary, where the predicted territory would be closer to the actual with Budapest as capital instead of Vienna. Overall, this suggests that capitals tend to be located such that they are well connected to their own territories, while keeping out of reach by other Great Powers.

The map in Figure A.14 shows how France's predicted territory changes when using Marseilles as capital instead of Paris. As seen, the predicted territory shows little semblance to the actual. Interestingly, northern France here becomes independent, rather than part of England or some other Great Power.

Online Appendix Tables and Figures

Across Cells and GP Pairs	Number of obs	Mean	Standard deviation	Minimum	Maximum
Battle Indicator	15950	0.026	0.158	0.0	1.0
Shortest-Distance Corridor Indicator	15950	0.026	0.160	0.0	1.0
Across Cells					
Sea Indicator	1450	0.612	0.488	0.0	1.0
Mountain Indicator ($>$ 800 meter)	1450	0.092	0.289	0.0	1.0
Marsh Indicator	1450	0.088	0.284	0.0	1.0
River Indicator	1450	0.397	0.489	0.0	1.0
Lake Indicator	1450	0.102	0.303	0.0	1.0
High-CSI Indicator (90th percentile)	1146	0.124	0.330	0.0	1.0
Across Land Cells (Sea Indicator = 0)					
Sea Indicator	563	0.000	0.000	0.0	0.0
Mountain Indicator ($>$ 800 meter)	563	0.165	0.372	0.0	1.0
Marsh Indicator	563	0.185	0.388	0.0	1.0
River Indicator	563	0.700	0.459	0.0	1.0
Lake Indicator	563	0.169	0.375	0.0	1.0
High-CSI Indicator (90th percentile)	563	0.188	0.391	0.0	1.0

Table A.1: Summary statistics for battle data variables.

	Correlations coefficients between the benchmark capital corridor indictor and indicators for two alternative corridors:	
Great Power pair	Non-capital corridors	Contour corridors
Austria-Germany	0.57	0.16
Austria-France	0.02	0.17
France-Germany	0.25	0.16
France-Russia	−0.05	0.16
France-Spain	−0.01	0.16
Spain-Austria	0.18	0.19
Ottoman-Austria	0.39	0.18
Ottoman-Russia	0.16	0.06
England-France	0.47	0.18
England-Russia	0.26	0.13
England-Spain	0.26	0.13

Notes: The table shows, for each Great Power pair, the correlation coefficients between our benchmark corridor measure between Great Power capitals and two alternative measures: between the largest non-capital cities, and around the states' contours.

Table A.2: Correlations between different corridors across Great Power pairs.

	Dependent variable is the Battle Indicator						
	(1)	(2)	(3)	(4)	(5)	(6)	(7)
SD Corridor Between Capitals	0.146***	0.145***	0.151***	0.124***	0.078***	0.069**	0.124**
	(0.019)	(0.019)	(0.019)	(0.017)	(0.020)	(0.032)	(0.047)
Corridors Around State Contours	0.074***	0.074***	0.076***	0.074***	0.048**	0.008	0.074***
	(0.006)	(0.006)	(0.006)	(0.006)	(0.019)	(0.061)	(0.016)
Sea Indicator		−0.013***	−0.013***		−0.049**		
		(0.003)	(0.003)		(0.020)		
Mountain Indicator (800 m)		−0.009**	−0.010**		−0.035		
		(0.004)	(0.004)		(0.036)		
Marsh Indicator		−0.010**	−0.009**		0.007		
		(0.004)	(0.004)		(0.032)		
R^2	0.06	0.06	0.07	0.23	0.19	0.61	0.23
Number of obs.	15950	15950	15950	15950	1379	1379	15950
Fixed effects	None	None	GP-pair	GP-pair, Cell	GP-pair	GP-pair, Cell	GP-pair, Cell
Sample	Full	Full	Full	Full	Cells $<$ 300 km of SD Corr.	Cells $<$ 300 km of SD Corr.	Full
Standard errors	Robust	Robust	Robust	Robust	Robust	Robust	Clustered

Notes: Variations on the regressions in Table 1, using two corridor indicators: the benchmark one referring to pairs of capitals, and the other referring to the contours of the GP's territories. Columns (5) and (6) restrict the sample to cells intersected by a 300 km buffer zone around the shortest-distance line between capitals. * indicates p <0.10, ** p <0.05, and *** p <0.01.

Table A.3: Controlling for contour corridors.

	Dependent variable is the Battle Indicator						
	(1)	(2)	(3)	(4)	(5)	(6)	(7)
SD Corridor Between Capitals	0.150***	0.149***	0.155***	0.127***	0.077***	0.067**	0.127**
	(0.019)	(0.019)	(0.019)	(0.017)	(0.020)	(0.032)	(0.045)
SD Corridor Between Non-Capitals	0.100***	0.099***	0.102***	0.100***	0.028	0.026	0.100***
	(0.017)	(0.017)	(0.016)	(0.015)	(0.023)	(0.044)	(0.030)
Sea Indicator		−0.010***	−0.010***		−0.041**		
		(0.003)	(0.003)		(0.019)		
Mountain Indicator (800 m)		−0.005	−0.005		−0.025		
		(0.005)	(0.004)		(0.036)		
Marsh Indicator		−0.017***	−0.017***		−0.006		
		(0.004)	(0.004)		(0.032)		
R^2	0.04	0.04	0.06	0.22	0.19	0.61	0.22
Number of obs.	15950	15950	15950	15950	1379	1379	15950
Fixed effects	None	None	GP-pair	GP-pair, Cell	GP-pair	GP-pair, Cell	GP-pair, Cell
Sample	Full	Full	Full	Full	Cells $<$ 300 km of SD Corr.	Cells $<$ 300 km of SD Corr.	Full
Standard errors	Robust	Robust	Robust	Robust	Robust	Robust	Clustered

Notes: Variations on the regressions in Table 1, using two corridor indicators: the benchmark one between pairs of capitals and the other between the largest non-capital cities (see text for details). Columns (5) and (6) restrict the sample to cells intersected by a 300 km buffer zone around the shortest-distance line between capitals. * indicates p <0.10, ** p <0.05, and *** p <0.01.

Table A.4: Controlling for non-capital corridors.

	Dependent variable is the Battle Indicator						
	(1)	(2)	(3)	(4)	(5)	(6)	(7)
SD Corridor Between Capitals	0.131***	0.130***	0.136***	0.110***	0.077***	0.066**	0.110**
	(0.019)	(0.019)	(0.019)	(0.017)	(0.020)	(0.032)	(0.045)
SD Corridor Between Non-Capitals	0.081***	0.079***	0.083***	0.082***	0.027	0.025	0.082**
	(0.016)	(0.016)	(0.016)	(0.015)	(0.023)	(0.044)	(0.031)
Corridors Around State Contours	0.069***	0.069***	0.071***	0.069***	0.048**	0.007	0.069***
	(0.006)	(0.006)	(0.006)	(0.006)	(0.019)	(0.061)	(0.016)
Sea Indicator		−0.013***	−0.012***		−0.050**		
		(0.003)	(0.003)		(0.020)		
Mountain Indicator (800 m)		−0.009*	−0.009*		−0.034		
		(0.004)	(0.004)		(0.036)		
Marsh Indicator		−0.009**	−0.009**		0.008		
		(0.004)	(0.004)		(0.032)		
R^2	0.07	0.07	0.08	0.24	0.19	0.61	0.24
Number of obs.	15950	15950	15950	15950	1379	1379	15950
Fixed effects	None	None	GP-pair	GP-pair, Cell	GP-pair	GP-pair, Cell	GP-pair, Cell
Sample	Full	Full	Full	Full	Cells < 300 km of SD Corr.	Cells < 300 km of SD Corr.	Full
Standard errors	Robust	Robust	Robust	Robust	Robust	Robust	Clustered

Notes: Variations on the regressions in Tables A.3 and A.4, but with all three corridor indicators: the benchmark one, the one between the largest non-capital cities, and the one around the GP' contours. * indicates p <0.10, ** p <0.05, and *** p <0.01.

Table A.5: Controlling for both non-capital and contour corridors.

	Dependent variable is the Battle Indicator						
	(1)	(2)	(3)	(4)	(5)	(6)	(7)
SD Corridor Between Capitals	0.146***	0.069**			0.127***	0.089*	0.099
	(0.017)	(0.032)			(0.017)	(0.049)	(0.086)
SD Corridor Between Non-Capitals			0.122***	0.056*	0.100***	0.053*	−0.043
			(0.015)	(0.029)	(0.015)	(0.029)	(0.089)
R^2	0.21	0.61	0.21	0.59	0.22	0.60	0.80
Number of obs.	15950	1379	15950	1555	15950	1555	792
Fixed effects	GP-pair, Cell	GP-pair, Cell	GP-pair, Cell	GP-pair, Cell	GP-pair, Cell	GP-pair, Cell	GP-pair, Cell
Sample	Full	$<$ 300km of Capital Corr.	Full	$<$ 300km of Non-Capital Corr.	Full	$<$ 300km of Non-Capital Corr.	$<$ 300km of Both Corridors
Standard errors	Robust	Robust	Robust	Robust	Robust	Robust	Robust

Notes: Various regressions with capital and non-capital corridors. Columns (1) and (2) reproduce columns (4) and (6) of Table 1; both use fixed effects for cells and GP pairs, and the latter restricts the sample to cells intersected by a 300 km buffer zone around the benchmark corridor between capitals. Columns (3) and (4) do the same as in columns (1) and (2) but for the non-capital corridor, with the sample in column (4) restricted to cells within 300 km of the non-capital corridor. Columns (5) and (6) do the same as in columns (3) and (4), but add the benchmark capital corridor as control. Column (7) does the same as in column (6) but restricts the sample to cells within 300 km of *both* corridors. * indicates p <0.10, ** p <0.05, and *** p <0.01.

Table A.6: Cells close to different corridors.

	Dependent variable is the Battle Indicator							
	(1)	(2)	(3)	(4)	(5)	(6)	(7)	(8)
Shortest-Distance Corridor	0.204***	0.158***	0.152***	0.060***	0.144***	0.148***	0.149***	0.149**
	(0.029)	(0.019)	(0.018)	(0.017)	(0.018)	(0.020)	(0.039)	(0.053)
Sea × SD-Corridor	−0.109***						−0.089**	−0.089
	(0.035)						(0.041)	(0.052)
Mountain × SD-Corridor		−0.120***					−0.203***	−0.203**
		(0.042)					(0.048)	(0.079)
Marsh × SD-Corridor			−0.072				−0.147***	−0.147*
			(0.047)				(0.052)	(0.077)
River × SD-Corridor				0.153***			0.142***	0.142**
				(0.032)			(0.035)	(0.052)
Lake × SD-Corridor					0.015		0.011	0.011
					(0.051)		(0.051)	(0.065)
High CSI × SD-Corridor						0.050	−0.015	−0.015
						(0.053)	(0.057)	(0.067)
R^2	0.21	0.21	0.21	0.22	0.21	0.21	0.22	0.22
Number of obs.	15950	15950	15950	15950	15950	12606	12606	12606
Fixed effects	GP-pair, Cell	GP-pair, Cell	GP-pair, Cell	GP-pair, Cell	GP-pair, Cell	GP-pair, Cell	GP-pair, Cell	GP-pair, Cell
Standard errors	Robust	Robust	Robust	Robust	Robust	Robust	Robust	Clustered

Notes: Similar ordinary least squares regressions as in Table 2, with cell and GP-pair fixed effects, and including more geography variables. * indicates p <0.10, ** p <0.05, and *** p <0.01.

Table A.7: More geography variables.

	Dependent variable is the Battle Indicator					
	(1)	(2)	(3)	(4)	(5)	(6)
Shortest-Distance Corridor Indicator	0.170***	0.201***	0.229***	0.248***	0.228***	0.220***
	(0.015)	(0.014)	(0.013)	(0.013)	(0.012)	(0.012)
Sea × SD-Corridor	−0.091***	−0.109***	−0.126***	−0.141***	−0.124***	−0.118***
	(0.017)	(0.016)	(0.016)	(0.016)	(0.016)	(0.016)
Mountain × SD-Corridor	0.096***	0.052***	−0.039*	−0.177***	−0.120***	−0.136**
	(0.018)	(0.020)	(0.023)	(0.028)	(0.035)	(0.064)
Marsh × SD-Corridor	−0.084***	−0.099***	−0.119***	−0.135***	−0.119***	−0.112***
	(0.030)	(0.030)	(0.030)	(0.030)	(0.029)	(0.029)
R^2	0.22	0.22	0.22	0.22	0.22	0.22
Number of obs.	15950	15950	15950	15950	15950	15950
Threshold for Mountain Indicator	200 m	400 m	600 m	800 m	1000 m	1500 m

Notes: The same ordinary least squares regressions as in column (6) of Table 2 but using different thresholds for what defines a mountain. All specifications include fixed effects for cells and Great Power pairs. Column (4) of this table replicates column (6) of Table 2. * indicates p <0.10, ** p <0.05, and *** p <0.01.

Table A.8: Different height thresholds for mountain indicator.

	Dependent variable is the Land Battle Indicator						
	(1)	(2)	(3)	(4)	(5)	(6)	(7)
Shortest-Distance Corridor Indicator	0.659***	0.464***	0.450***	0.807***	0.809***	0.700***	0.700**
	(0.113)	(0.070)	(0.069)	(0.140)	(0.139)	(0.125)	(0.246)
Sea Indicator	−0.010			−0.016**	−0.017**		
	(0.006)			(0.007)	(0.007)		
Mountain Indicator (800 m)		0.002		−0.005	−0.006		
		(0.010)		(0.012)	(0.011)		
Marsh Indicator			−0.026***	−0.034***	−0.035***		
			(0.005)	(0.007)	(0.007)		
Sea × SD-Corridor	−0.433***			−0.540***	−0.524***	−0.482***	−0.482**
	(0.130)			(0.145)	(0.143)	(0.130)	(0.210)
Mountain × SD-Corridor		−0.355***		−0.578***	−0.566***	−0.533***	−0.533**
		(0.103)		(0.136)	(0.134)	(0.123)	(0.210)
Marsh × SD-Corridor			−0.253*	−0.477***	−0.464***	−0.443***	−0.443*
			(0.131)	(0.158)	(0.156)	(0.130)	(0.214)
R^2	0.03	0.03	0.03	0.04	0.05	0.22	0.22
Number of obs.	15950	15950	15950	15950	15950	15950	15950
Fixed effects	None	None	None	None	GP-pair	GP-pair, Cell	GP-pair, Cell
Standard errors	Robust	Robust	Robust	Robust	Robust	Robust	Clustered

Notes: The same ordinary least squares regressions as in Table 2 but using a Land Battle Indicator as dependent variable. * indicates p <0.10, ** p <0.05, and *** p <0.01.

Table A.9: Only land battles.

	Dependent variable is the Battle Indicator						
	(1)	(2)	(3)	(4)	(5)	(6)	(7)
Shortest-Distance Corridor Indicator	0.175***	0.133***	0.136***	0.225***	0.229***	0.190***	0.190**
	(0.036)	(0.022)	(0.022)	(0.043)	(0.043)	(0.040)	(0.068)
Sea Indicator	−0.003			−0.005*	−0.005*		
	(0.002)			(0.003)	(0.003)		
Mountain Indicator (800 m)		0.001		−0.001	−0.001		
		(0.004)		(0.004)	(0.004)		
Marsh Indicator			−0.009***	−0.011***	−0.011***		
			(0.003)	(0.004)	(0.004)		
Sea × SD-Corridor	−0.089**			−0.126***	−0.124***	−0.097**	−0.097
	(0.043)			(0.047)	(0.047)	(0.044)	(0.059)
Mountain × SD-Corridor		−0.108**		−0.148***	−0.141***	−0.146***	−0.146**
		(0.050)		(0.051)	(0.051)	(0.051)	(0.061)
Marsh × SD-Corridor			−0.148***	−0.220***	−0.219***	−0.203***	−0.203***
			(0.023)	(0.039)	(0.039)	(0.039)	(0.051)
R^2	0.01	0.01	0.01	0.02	0.03	0.19	0.19
Number of obs.	15626	15626	15626	15626	15626	15626	15626
Fixed effects	None	None	None	None	GP-pair	GP-pair, Cell	GP-pair, Cell
Standard errors	Robust	Robust	Robust	Robust	Robust	Robust	Clustered

Notes: The same ordinary least squares regressions as in Table 2 but dropping those observations that are closer than 200 km from anyone of the relevant capitals for each pair. * indicates p <0.10, ** p <0.05, and *** p <0.01.

Table A.10: Dropping observations close to capitals.

	Dependent variable is the Battle Indicator						
	(1)	(2)	(3)	(4)	(5)	(6)	(7)
Shortest-Distance Corridor Indicator	0.230***	0.197***	0.193***	0.262***	0.265***	0.239***	0.239***
	(0.028)	(0.021)	(0.021)	(0.031)	(0.031)	(0.029)	(0.055)
Sea Indicator	−0.003			−0.005	−0.005*		
	(0.002)			(0.003)	(0.003)		
Mountain Indicator (800 m)		0.002		−0.000	−0.000		
		(0.004)		(0.004)	(0.004)		
Marsh Indicator			−0.010***	−0.013***	−0.013***		
			(0.003)	(0.004)	(0.004)		
Sea × SD-Corridor	−0.104***			−0.121***	−0.116***	−0.120***	−0.120**
	(0.038)			(0.038)	(0.038)	(0.035)	(0.046)
Mountain × SD-Corridor		−0.119**		−0.158***	−0.154***	−0.173***	−0.173**
		(0.052)		(0.053)	(0.052)	(0.044)	(0.068)
Marsh × SD-Corridor			−0.079	−0.114**	−0.108*	−0.115**	−0.115
			(0.056)	(0.058)	(0.057)	(0.049)	(0.065)
R^2	0.04	0.04	0.04	0.04	0.06	0.22	0.22
Number of obs.	15950	15950	15950	15950	15950	15950	15950
Fixed effects	None	None	None	None	GP-pair	GP-pair, Cell	GP-pair, Cell
Standard errors	Robust	Robust	Robust	Robust	Robust	Robust	Clustered

Notes: The same ordinary least squares regressions as in Table 2 but based on a dataset where Moscow is assigned as the Russian capital instead of St Petersburg. * indicates p <0.10, ** p <0.05, and *** p <0.01.

Table A.11: Moscow as Russia's capital instead of St Petersburg.

	Dependent variable is the Battle Indicator						
	(1)	(2)	(3)	(4)	(5)	(6)	(7)
Shortest-Distance Corridor Indicator	0.099***	0.080***	0.078***	0.108***	0.113***	0.089***	0.089**
	(0.014)	(0.010)	(0.009)	(0.016)	(0.015)	(0.015)	(0.038)
Sea Indicator	−0.002			−0.003**	−0.003**		
	(0.001)			(0.002)	(0.002)		
Mountain Indicator (800 m)		0.001		−0.000	−0.000		
		(0.002)		(0.002)	(0.002)		
Marsh Indicator			−0.005***	−0.007***	−0.007***		
			(0.002)	(0.002)	(0.002)		
Sea × SD-Corridor	−0.046**			−0.050***	−0.050***	−0.034*	−0.034
	(0.018)			(0.018)	(0.018)	(0.018)	(0.030)
Mountain × SD-Corridor		−0.043		−0.057**	−0.057**	−0.064***	−0.064*
		(0.026)		(0.027)	(0.026)	(0.024)	(0.032)
Marsh × SD-Corridor			−0.019	−0.032	−0.033	−0.051*	−0.051
			(0.033)	(0.034)	(0.033)	(0.029)	(0.044)
R^2	0.01	0.01	0.01	0.02	0.04	0.13	0.13
Number of obs.	30450	30450	30450	30450	30450	30450	30450
Fixed effects	None	None	None	None	GP-pair	GP-pair, Cell	GP-pair, Cell
Standard errors	Robust	Robust	Robust	Robust	Robust	Robust	Clustered

Notes: The same ordinary least squares regressions as in Table 2 but based on all 21 GP pairs, including those that fought less than 10 battles. * indicates p <0.10, ** p <0.05, and *** p <0.01.

Table A.12: Interactions with geography: all 21 pairs.

	Dependent variable is Number of Battles						
	(1)	(2)	(3)	(4)	(5)	(6)	(7)
Shortest-Distance Corridor Indicator	0.654***	0.473***	0.460***	0.803***	0.807***	0.696***	0.696**
	(0.113)	(0.070)	(0.069)	(0.140)	(0.139)	(0.125)	(0.243)
Sea Indicator	−0.005			−0.011	−0.011		
	(0.006)			(0.007)	(0.007)		
Mountain Indicator (800 m)		−0.003		−0.008	−0.009		
		(0.010)		(0.011)	(0.011)		
Marsh Indicator			−0.025***	−0.030***	−0.030***		
			(0.007)	(0.008)	(0.008)		
Sea × SD-Corridor	−0.407***			−0.515***	−0.499***	−0.455***	−0.455*
	(0.131)			(0.145)	(0.144)	(0.130)	(0.211)
Mountain × SD-Corridor		−0.363***		−0.578***	−0.567***	−0.532***	−0.532**
		(0.104)		(0.135)	(0.134)	(0.122)	(0.207)
Marsh × SD-Corridor			−0.267**	−0.485***	−0.471***	−0.443***	−0.443*
			(0.131)	(0.158)	(0.156)	(0.130)	(0.212)
R^2	0.03	0.03	0.03	0.04	0.05	0.21	0.21
Number of obs.	15950	15950	15950	15950	15950	15950	15950
Fixed effects	None	None	None	None	GP-pair	GP-pair, Cell	GP-pair, Cell
Standard errors	Robust	Robust	Robust	Robust	Robust	Robust	Clustered

Notes: The same ordinary least squares regressions as in Table 2, but using the *number* of battles (in each cell and between the relevant pair) as the dependent variable. * indicates p <0.10, ** p <0.05, and *** p <0.01.

Table A.13: Number of battles as dependent variable.

	Dependent variable is the Battle Indicator					
	(1)	(2)	(3)	(4)	(5)	(6)
Shortest-Distance Corridor Indicator	0.248***	0.248***	0.248***	0.248***	0.248***	0.248***
	(0.034)	(0.043)	(0.050)	(0.053)	(0.056)	(0.058)
Sea × SD-Corridor	−0.141***	−0.141***	−0.141***	−0.141***	−0.141***	−0.141***
	(0.037)	(0.042)	(0.043)	(0.045)	(0.049)	(0.051)
Mountain × SD-Corridor	−0.177***	−0.177***	−0.177***	−0.177***	−0.177***	−0.177***
	(0.045)	(0.054)	(0.047)	(0.045)	(0.043)	(0.045)
Marsh × SD-Corridor	−0.135**	−0.135*	−0.135	−0.135	−0.135*	−0.135*
	(0.053)	(0.080)	(0.090)	(0.085)	(0.076)	(0.069)
R^2	0.22	0.22	0.22	0.22	0.22	0.22
Number of obs.	15950	15950	15950	15950	15950	15950
Distance cut-off	0 km	200 km	400 km	600 km	800 km	1000 km

Notes: Ordinary least squares regressions with spatially adjusted standard errors and declining weights (the Bartlett option in acreg). All specifications include Cell and Great Power pair fixed effects. Column (1) replicates the results in Table 2, column (6), with robust standard errors now adjusted for spatial correlation. * indicates p <0.10, ** p <0.05, and *** p <0.01.

Table A.14: Spatially adjusted standard errors.

	Dependent variable is the Battle Indicator					
	(1)	(2)	(3)	(4)	(5)	(6)
Shortest-Distance Corridor Indicator	0.200***	0.220***	0.217***	0.205***	0.203***	0.179***
	(0.035)	(0.035)	(0.035)	(0.035)	(0.035)	(0.036)
Sea × SD-Corridor	−0.119***	−0.128***	−0.127***	−0.124***	−0.124***	−0.115***
	(0.038)	(0.038)	(0.038)	(0.038)	(0.037)	(0.038)
Mountain × SD-Corridor	−0.163***	−0.169***	−0.175***	−0.172***	−0.175***	−0.162***
	(0.046)	(0.046)	(0.046)	(0.046)	(0.046)	(0.046)
Marsh × SD-Corridor	−0.110**	−0.120**	−0.119**	−0.112**	−0.121**	−0.110**
	(0.052)	(0.052)	(0.052)	(0.052)	(0.051)	(0.052)
City × SD-Corridor	0.116***	0.081*	0.079*	0.103**	0.103***	0.116***
	(0.044)	(0.048)	(0.044)	(0.042)	(0.040)	(0.036)
R^2	0.22	0.22	0.22	0.22	0.22	0.22
Number of obs.	15950	15950	15950	15950	15950	15950
Year in which city presence measured	1300	1400	1500	1600	1700	1800

Notes: Ordinary least squares regressions with robust standard errors. The variable City × SD-Corridor is an interaction term defined as the product of a City Indicator and the SD-corridor Indicator. The City Indicator equals one for cells having a city with population above 5,000 in the year indicated. All specifications include both Cell and Great Power pair fixed effects. * indicates p <0.10, ** p <0.05, and *** p <0.01.

Table A.15: City presence.

	Dependent variable is the Battle Indicator						
	(1)	(2)	(3)	(4)	(5)	(6)	(7)
Shortest-Distance Corridor Indicator	0.117***	0.136***	0.143***	0.132***	0.132***	0.136***	0.136**
	(0.026)	(0.022)	(0.024)	(0.030)	(0.030)	(0.028)	(0.046)
Sea Indicator	−0.004			−0.003	−0.003		
	(0.003)			(0.004)	(0.003)		
Mountain Indicator (800 m)		0.001		0.000	0.000		
		(0.005)		(0.005)	(0.005)		
Marsh Indicator			0.006	0.004	0.004		
			(0.005)	(0.006)	(0.006)		
Sea × SD-Corridor	0.041			0.034	0.038	0.010	0.010
	(0.045)			(0.047)	(0.046)	(0.044)	(0.048)
Mountain × SD-Corridor		−0.157***		−0.160***	−0.139***	−0.152***	−0.152**
		(0.022)		(0.027)	(0.026)	(0.058)	(0.045)
Marsh × SD-Corridor			−0.068	−0.066	−0.062	−0.072	−0.072
			(0.053)	(0.055)	(0.053)	(0.055)	(0.073)
R^2	0.02	0.02	0.02	0.02	0.04	0.27	0.27
Number of obs.	8820	8820	8820	8820	8820	8820	8820
Fixed effects	None	None	None	None	GP-pair	GP-pair, Cell	GP-pair, Cell
Standard errors	Robust	Robust	Robust	Robust	Robust	Robust	Clustered

Notes: The same ordinary least squares regressions as in Table 2, but using battles over the period 1914-1945, instead of 1525-1913. * indicates p <0.10, ** p <0.05, and *** p <0.01.

Table A.16: Battles 1914-1945.

Across Capital City Pairs	Number of obs	Mean	Standard deviation	Minimum	Maximum
Length of Corridor	435	1.338	0.664	0.12	3.62
Fra Sea Along Corr.	435	0.224	0.222	0.00	0.94
Fra Mountain Along Corr.	435	0.105	0.113	0.00	0.65
Fra Marsh Along Corr.	435	0.002	0.005	0.00	0.06
Separatedness Index	435	0.054	0.035	0.00	0.15
Across Non-Capital City Pairs					
Length of Corridor	221445	1.329	0.761	0.00	4.55
Fra Sea Along Corr.	221445	0.245	0.240	0.00	0.99
Fra Mountain Along Corr.	221445	0.136	0.124	0.00	1.00
Fra Marsh Along Corr.	221445	0.001	0.002	0.00	0.09
Separatedness Index	221445	0.062	0.038	0.00	0.17

Table A.17: Summary statistics for city data variables.

	Dependent variable is the Geodesic Distance Between Non-Capitals						
	(1)	(2)	(3)	(4)	(5)	(6)	(7)
Fraction Sea	0.163***			0.317***		0.317	
	(0.009)			(0.011)		(0.196)	
Fraction Mountain		0.305***		0.579***		0.579*	
		(0.022)		(0.026)		(0.312)	
Fraction Marsh			−4.327***	−0.424		−0.424	
			(0.747)	(0.806)		(4.195)	
Separatedness Index					2.065***		2.065*
					(0.071)		(1.211)
R^2	0.46	0.46	0.46	0.46	0.46	0.46	0.46
Number of obs.	221445	221445	221445	221445	221445	221445	221445
Standard errors	Robust	Robust	Robust	Robust	Robust	Clustered	Clustered

Notes: The same regressions as in Table 3, but for pairs of cities, such that none of them is a capital according to Bosker et al. (2013). All specifications include city fixed effects. * indicates p <0.10, ** p <0.05, and *** p <0.01.

Table A.18: Geodesic distance between non-capitals.

	Dependent variable is the Geodesic Distance Between Capitals or Non-Capitals							
	(1)	(2)	(3)	(4)	(5)	(6)	(7)	(8)
Separatedness Index	−4.068**	−0.476	−4.068**	−0.301	−4.439**	2.472	−3.814	2.713
	(1.677)	(1.141)	(1.677)	(1.117)	(1.943)	(2.257)	(2.315)	(4.836)
R^2	0.56	0.49	0.56	0.57	0.55	0.63	0.66	0.57
Number of obs.	378	37950	378	12403	276	1176	153	136
Capitals/non-capitals	Capitals	Non-capitals	Capitals	Non-capitals	Capitals	Non-capitals	Capitals	Non-capitals
Percentile pop. size	50%	50%	75%	75%	90%	90%	95%	95%

Notes: Regressions similar to those in Table 3, but considering capitals and non-capitals, and restricting the samples to observations where both cities in the pair have populations above the median (50th percentile), and in the 75th, 90th, and 95th percentiles of the full sample; the associated population levels (in thousands) are 15, 20, 40, and 76, respectively. The population data are from Bosker et al. (2013). The capitals/non-capitals samples are explained in Table A.20, here based on the definition in Bosker et al. (2013). Standard errors, reported in parentheses, are clustered on cell pairs throughout. All specifications also include city fixed effects. * indicates p <0.10, ** p <0.05, and *** p <0.01.

Table A.19: Big cities.

	Dependent variable is the Geodesic Distance Between Capitals					
	(1)	(2)	(3)	(4)	(5)	(6)
Separatedness Index	-4.973^{***}	-8.459^{***}	-2.480	-4.973^{***}	-8.459^{***}	-2.480
	(1.373)	(2.452)	(4.717)	(1.590)	(2.528)	(4.670)
R^2	0.52	0.72	0.70	0.52	0.72	0.70
Number of obs.	435	45	21	435	45	21
Definition of capitals	Bosker	Great Pwrs (broad)	Great Pwrs (narrow)	Bosker	Great Pwrs (broad)	Great Pwrs (narrow)
Standard errors	Robust	Robust	Robust	Clustered	Clustered	Clustered

Notes: Some variations on the regressions presented in Table 3, based on the Seperatedness Index and using different definitions of capitals. Standard errors are reported in parentheses: robust in columns (1)-(3), and clustered on cell pairs in columns (4)-(6). All specifications include city fixed effects. * indicates $p < 0.10$, ** $p < 0.05$, and *** $p < 0.01$.

Table A.20: Alternative definitions of capitals.

	Dependent variable is the Same-State Indicator in 2000						
	(1)	(2)	(3)	(4)	(5)	(6)	(7)
Length of Corridor	−0.255***	−0.256***	−0.258***	−0.247***	−0.248***	−0.247***	−0.248***
	(0.001)	(0.001)	(0.001)	(0.001)	(0.001)	(0.018)	(0.018)
Fra Sea along Corr.	−0.336***			−0.515***		−0.515***	
	(0.003)			(0.004)		(0.049)	
Fra Mountain along Corr.		−0.220***		−0.667***		−0.667***	
		(0.007)		(0.008)		(0.132)	
Fra Marsh along Corr.			1.443***	−3.855***		−3.855*	
			(0.336)	(0.366)		(2.210)	
Separatedness Index					−3.194***		−3.194***
					(0.022)		(0.310)
R^2	0.28	0.24	0.24	0.31	0.31	0.31	0.31
Number of obs.	241860	241860	241860	241860	241860	241860	241860
Standard errors	Robust	Robust	Robust	Robust	Robust	Clustered	Clustered

Notes: The same regressions as in Table 4, except that the dependent variable is an indicator for the pair of cities belonging to the same state in 2000, based on maps from Euratlas. All specifications include city fixed effects. * indicates p <0.10, ** p <0.05, and *** p <0.01.

Table A.21: Euratlas borders for 2000.

	Dependent variable is the Same-State Indicator based on the most recent GADM borders						
	(1)	(2)	(3)	(4)	(5)	(6)	(7)
Length of Corridor	−0.253***	−0.254***	−0.256***	−0.245***	−0.246***	−0.245***	−0.246***
	(0.001)	(0.001)	(0.001)	(0.001)	(0.001)	(0.018)	(0.018)
Fra Sea along Corr.	−0.333***			−0.510***		−0.510***	
	(0.003)			(0.004)		(0.049)	
Fra Mountain along Corr.		−0.219***		−0.661***		−0.661***	
		(0.007)		(0.008)		(0.132)	
Fra Marsh along Corr.			1.653***	−3.594***		−3.594	
			(0.336)	(0.365)		(2.189)	
Separatedness Index					−3.167***		−3.167***
					(0.022)		(0.309)
R^2	0.27	0.24	0.24	0.31	0.31	0.31	0.31
Number of obs.	241860	241860	241860	241860	241860	241860	241860
Standard errors	Robust	Robust	Robust	Robust	Robust	Clustered	Clustered

Notes: The same regressions as in Table 4, except that the dependent variable is an indicator for the pair of cities belonging to the same state in modern times, based on the most recent borders from the Global Administrative Areas (GADM). All specifications include city fixed effects. * indicates p <0.10, ** p <0.05, and *** p <0.01.

Table A.22: State borders from GADM.

	The dependent variable is the Same-State Indicator for different years									
	(1)	(2)	(3)	(4)	(5)	(6)	(7)	(8)	(9)	(10)
Length of Corridor	−0.181***	−0.267***	−0.197***	−0.190***	−0.121***	−0.149***	−0.180***	−0.278***	−0.264***	−0.375***
	(0.032)	(0.029)	(0.027)	(0.025)	(0.018)	(0.028)	(0.032)	(0.025)	(0.026)	(0.030)
Fra Sea along Corr.	−0.263*	−0.176	−0.008	0.132	−0.254***	−0.240**	−0.304**	−0.045	0.068	0.095
	(0.141)	(0.153)	(0.130)	(0.129)	(0.094)	(0.115)	(0.136)	(0.159)	(0.182)	(0.152)
Fra Mountain along Corr.	−0.594***	−0.227	−0.696***	−0.336	−0.891***	−0.639***	−0.732***	−0.438**	−0.421*	−0.583**
	(0.221)	(0.227)	(0.209)	(0.228)	(0.140)	(0.207)	(0.232)	(0.201)	(0.232)	(0.240)
Fra Marsh along Corr.	−9.984*	1.606	−9.745*	−8.001*	−11.427***	−3.360	−4.762	6.269	8.127	0.063
	(5.513)	(6.408)	(5.005)	(4.333)	(3.662)	(6.864)	(6.945)	(7.283)	(7.092)	(6.513)
R^2	0.38	0.41	0.41	0.34	0.40	0.35	0.37	0.47	0.43	0.65
Number of obs.	946	1035	946	990	990	780	861	741	630	780
Year in which state borders are measured	900	1000	1100	1200	1300	1400	1500	1600	1700	1800

Notes: Ordinary least squares regressions with standard errors in parentheses, clustered on 5 × 5-degree cell pairs. The unit of observation is a pair of cities that existed both in 800 CE and in the year in which outcomes are measured. The dependent variable is an indicator for whether the two cities belonged to the same state in the years indicated. All specifications include city fixed effects. * indicates p <0.10, ** p <0.05, and *** p <0.01.

Table A.23: City pairs in 800 CE and same-state outcomes by century.

	The dependent variable is the Same-State Indicator for different years									
	(1)	(2)	(3)	(4)	(5)	(6)	(7)	(8)	(9)	(10)
Length of Corridor	-0.171^{***}	-0.266^{***}	-0.180^{***}	-0.179^{***}	-0.110^{***}	-0.144^{***}	-0.175^{***}	-0.273^{***}	-0.260^{***}	-0.369^{***}
	(0.035)	(0.029)	(0.032)	(0.029)	(0.023)	(0.031)	(0.036)	(0.022)	(0.025)	(0.030)
Separatedness Index	-2.074^{**}	-1.163	-1.060	0.191	-2.424^{***}	-1.900^{**}	-2.351^{**}	-0.777	-0.065	-0.043
	(0.916)	(0.945)	(0.938)	(0.933)	(0.690)	(0.805)	(0.961)	(0.932)	(1.117)	(0.961)
R^2	0.36	0.41	0.35	0.31	0.32	0.32	0.35	0.46	0.41	0.62
Number of obs.	946	1035	946	990	990	780	861	741	630	780
Year in which state borders are measured	900	1000	1100	1200	1300	1400	1500	1600	1700	1800

Notes: The same ordinary least squares regressions as in Table A.23 but with the Separatedness Index as the independent variable of interest, instead of entering the three geography variables separately. * indicates $p < 0.10$, ** $p < 0.05$, and *** $p < 0.01$.

Table A.24: City pairs in 800 CE and same-state outcomes using the seperatedness index.

Great Power	Ratio of predicted to actual territory	Overlap ratio (predicted *and* actual territory over predicted *or* actual territory)	
		Using actual GP capital	Using alternative GP capital
England	0.96	0.96	0.94
France	0.79	0.53	0.24
Germany	0.81	0.53	0.48
Austria-Hungary	0.71	0.46	0.68
Spain	1.17	0.82	0.70
Ottoman Empire	2.69	0.36	0.30

Notes: The first column shows predicted territory over actual territory (i.e., the number of cities predicted to belong to the same state as the GP's capital divided by the number of cities actually belonging to that GP in 1900). The second and third columns show the overlap ratio, defined as (1) the size of the *intersection* of the predicted and actual territories, divided by (2) the size of the *union* of the predicted and actual territories; this ratio always falls between 0 and 1 (see Figure A.13). The second column uses the actual capital to predict territories (e.g., London for England) and the third column uses an alternative city (e.g., Manchester for England).

Table A.25: Comparing actual and predicted territories of Great Powers.

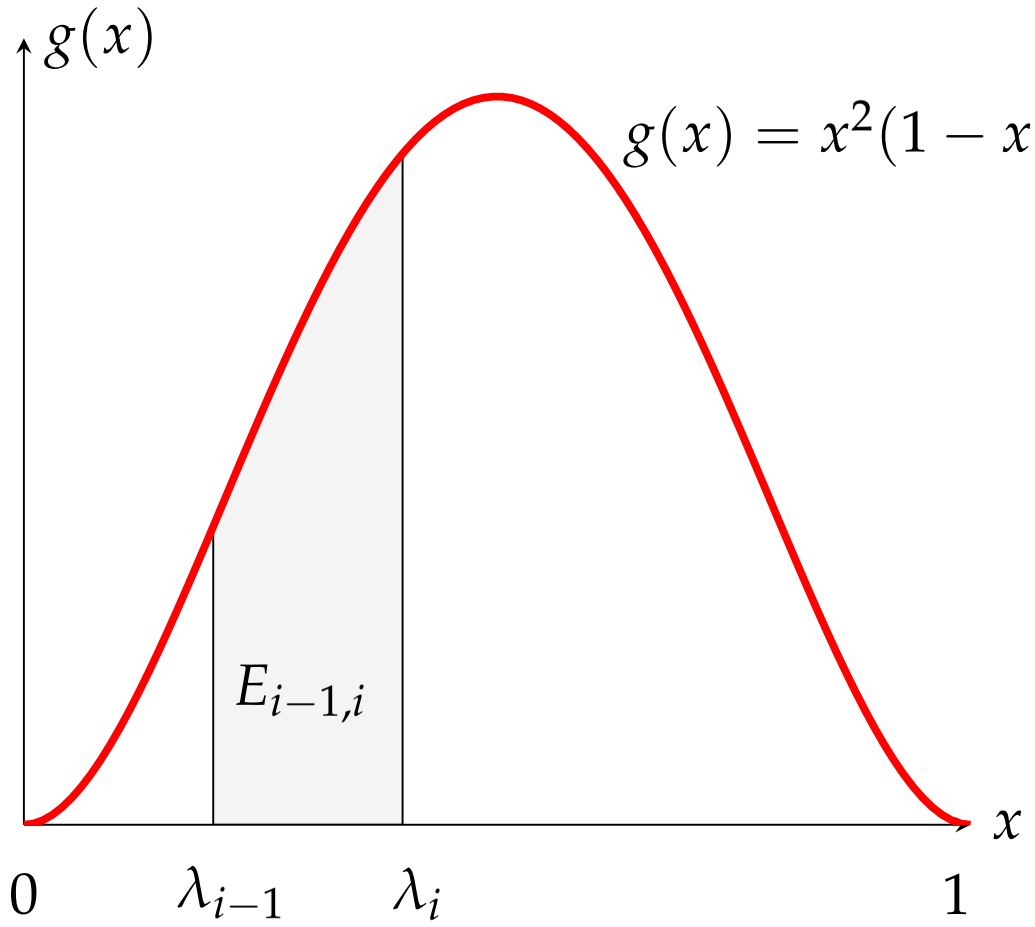

Figure A.1: Illustration of geodesic distance ($\lambda_i - \lambda_{i-1}$) and effective distance ($E_{i-1,i}$) in a world with $g(x) = x^2(1-x)^2$.

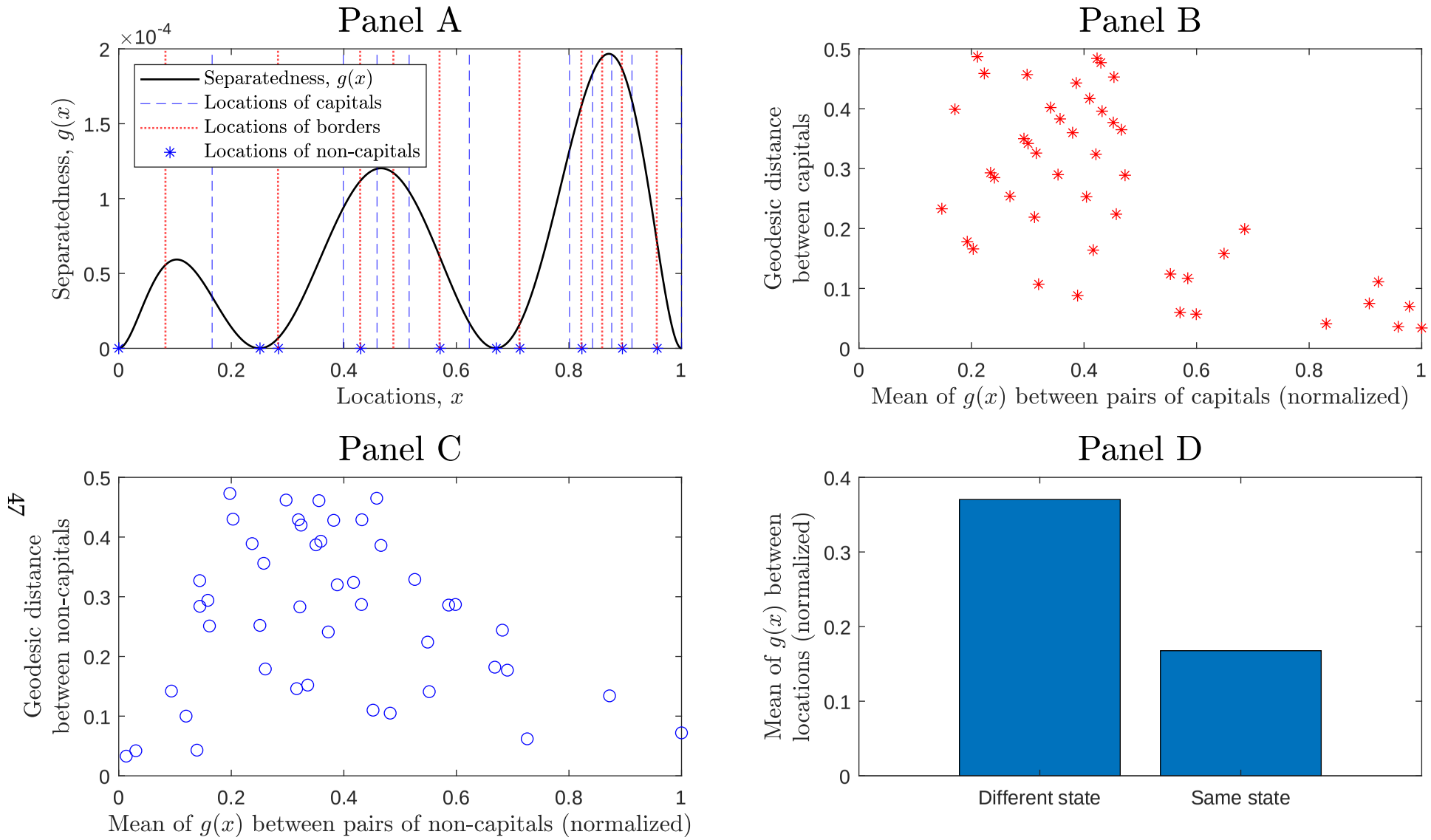

Figure A.2: Model illustration with $g(x) = x^2(1-x)^2(x-1/4)^2(x-2/3)^2$.

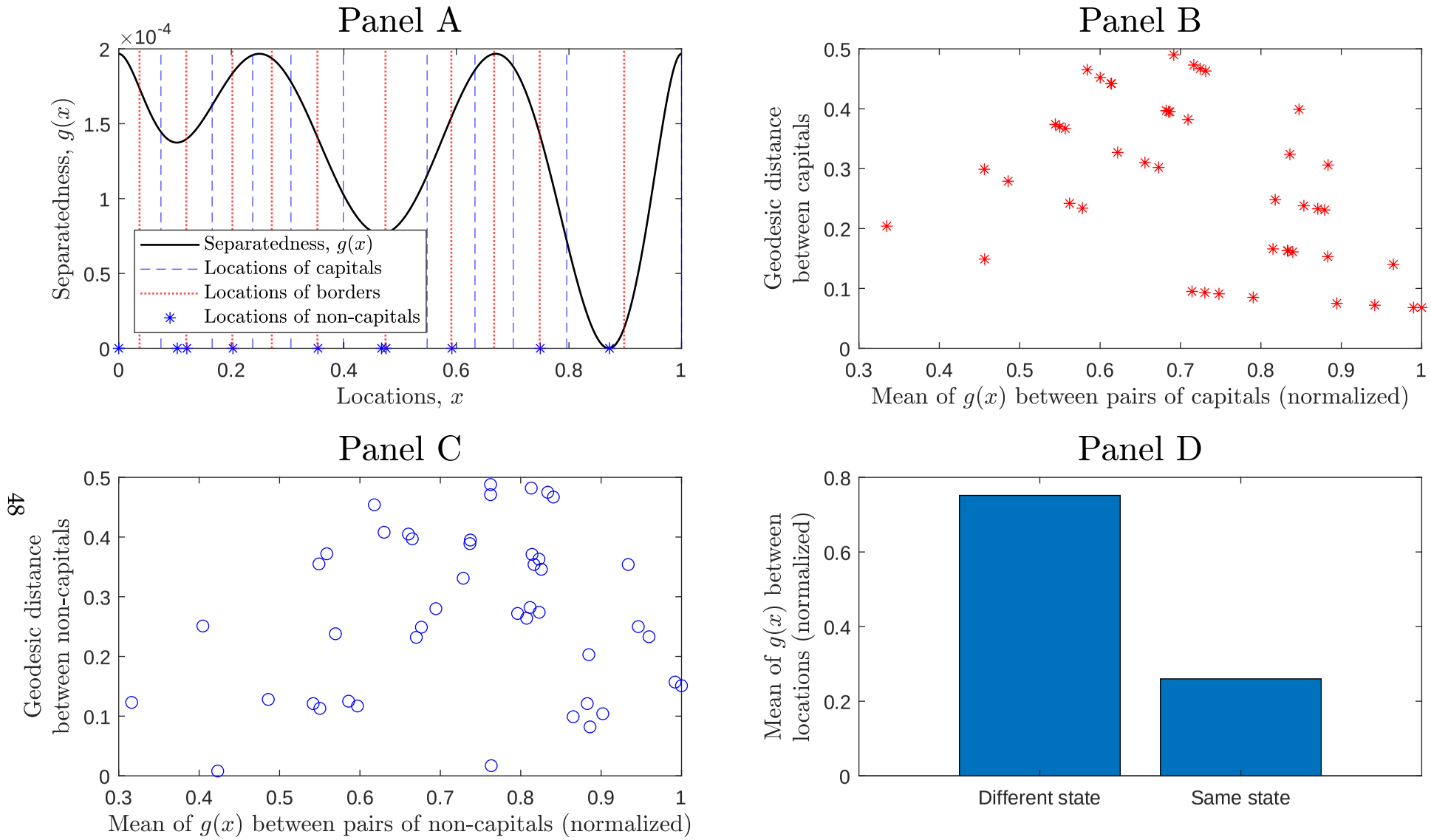

Figure A.3: Model illustration using a geography like that in Figure A.2, but inverted (see text).

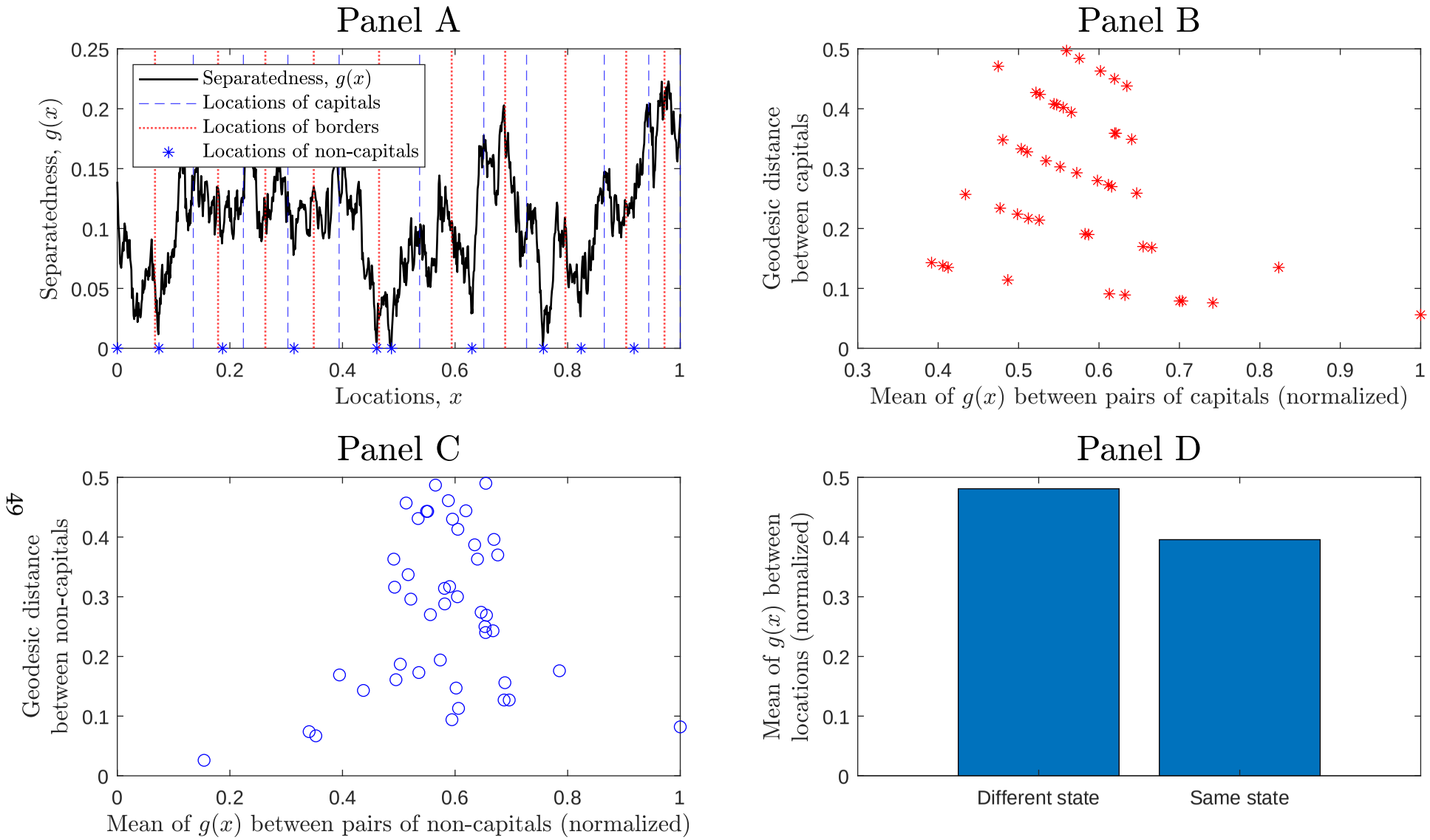

Figure A.4: Model illustration with a randomized geography.

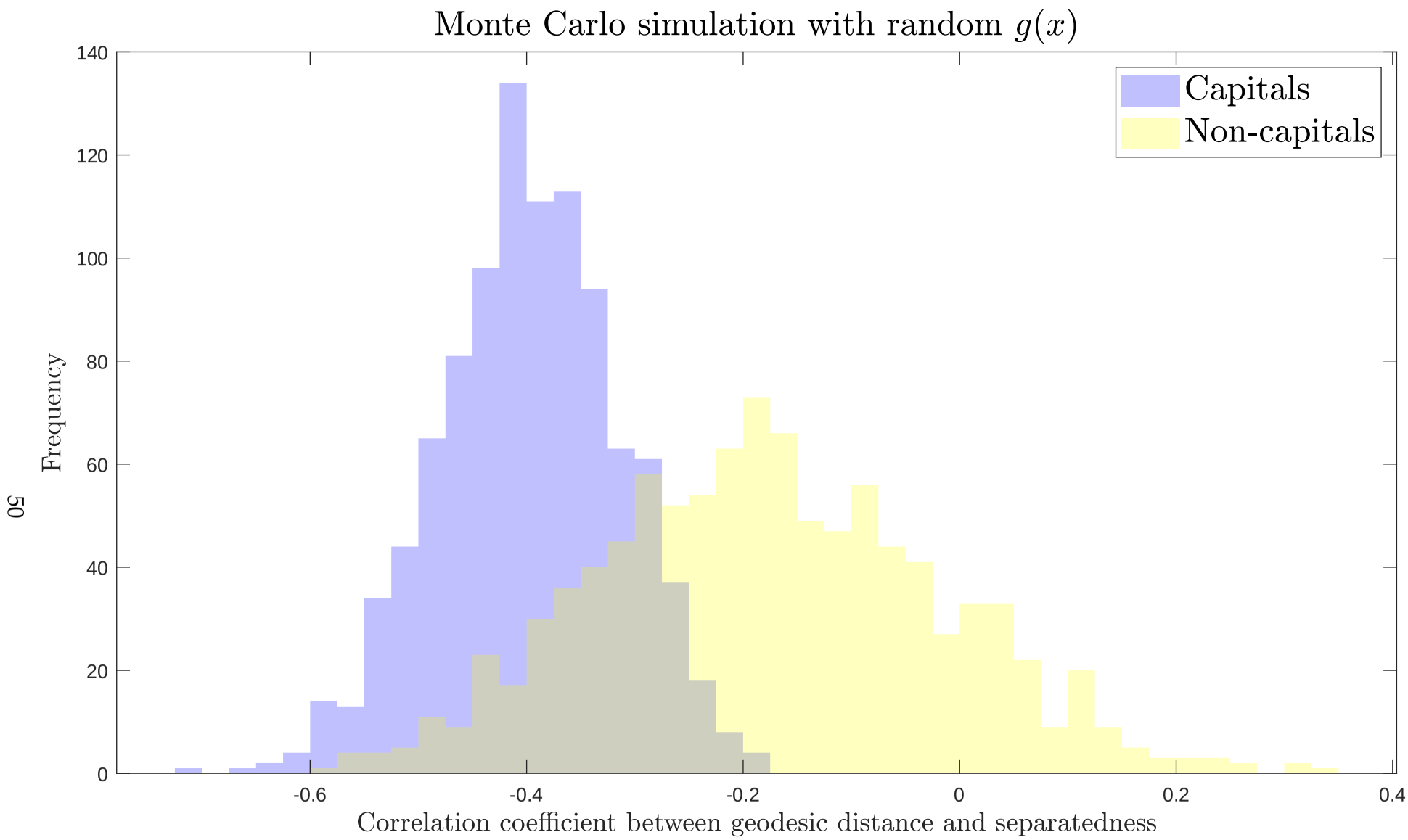

Figure A.5: Monte Carlo simulation with 5,000 randomized geographies.

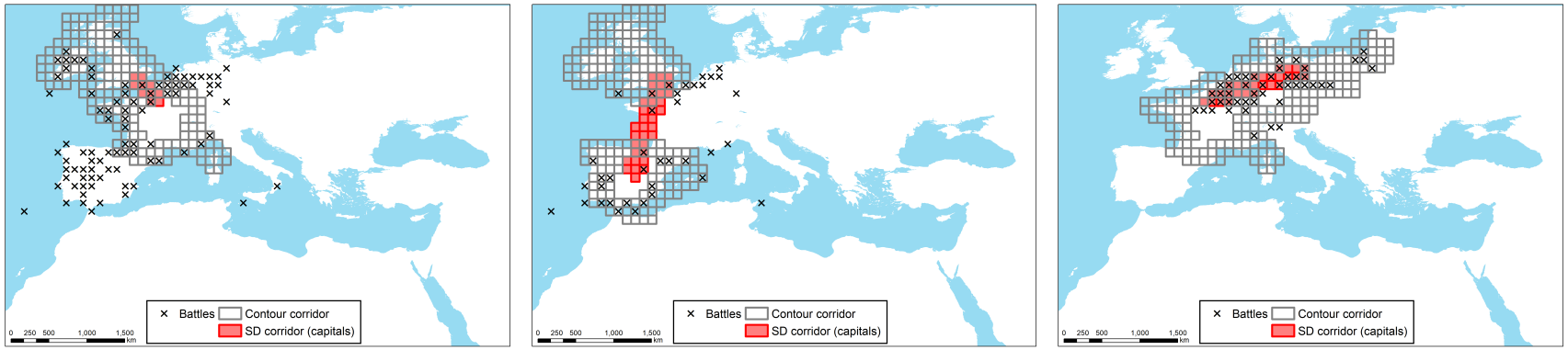

(a) England vs. France **(b)** England vs. Spain **(c)** France vs. Germany

(d) Ottoman Empire vs. Austria **(e)** France vs. Russia **(f)** Austria vs. Spain

Figure A.6: Corridors around the contours of Great Power territories in 1900, and the corresponding benchmark corridors between capitals. We consider the same six pairs as in Figure 2.

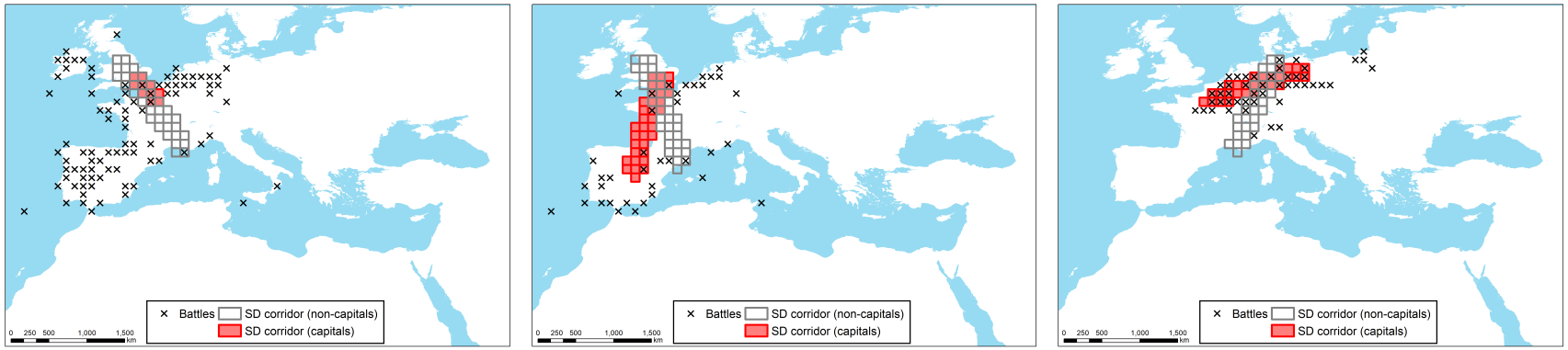

(a) England vs. France **(b)** England vs. Spain **(c)** France vs. Germany

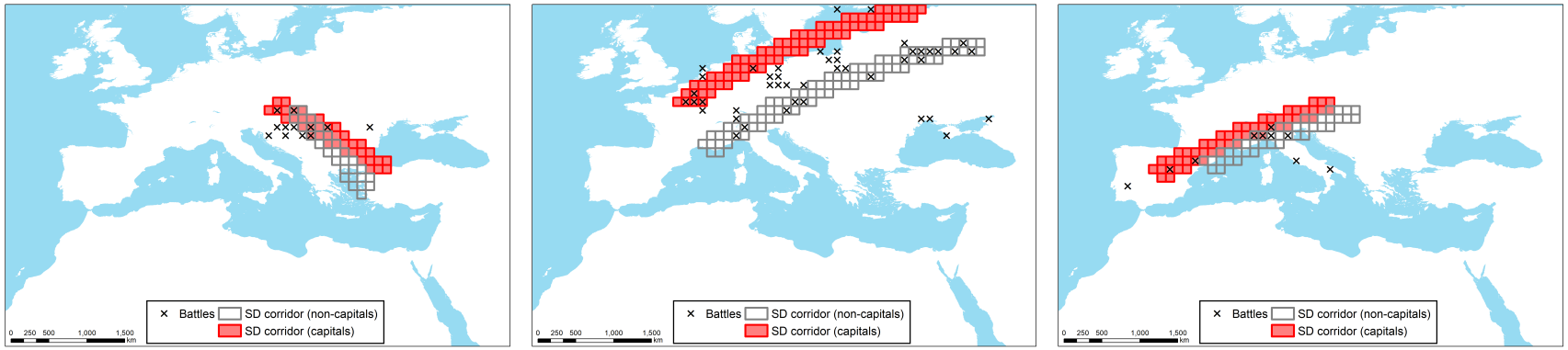

(d) Ottoman Empire vs. Austria **(e)** France vs. Russia **(f)** Austria vs. Spain

Figure A.7: Benchmark corridors between capitals and the corresponding non-capital corridors based on Barcelona, Budapest, Izmir/Smyrna, Manchester, Marseilles, and Moscow. We consider the same six pairs as in Figure 2.

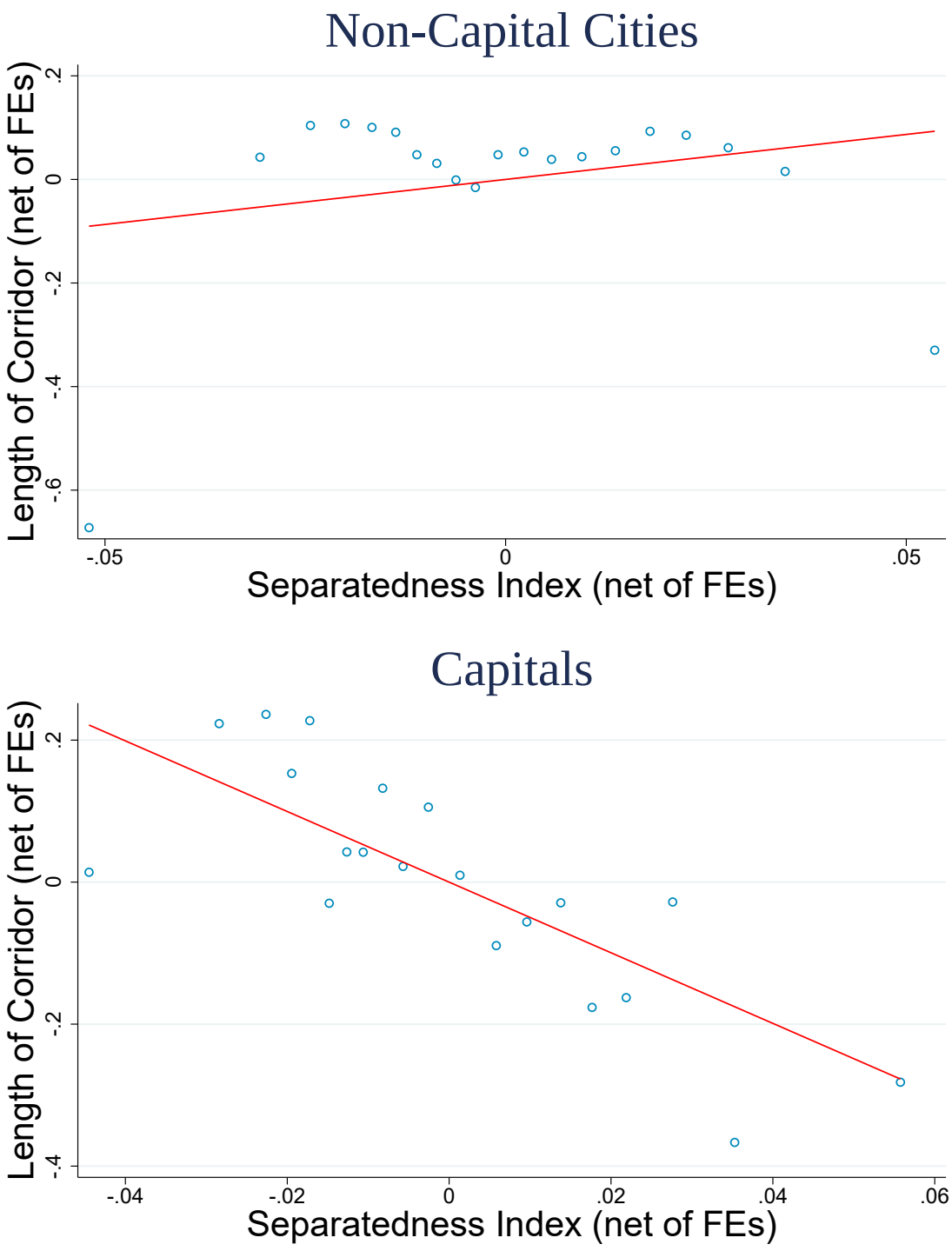

Figure A.8: Binscatter plots contrasting the different relationships between geodesic distance and separatedness for non-capital cities and capitals, based on the definition of capitals from Bosker et al. (2013).

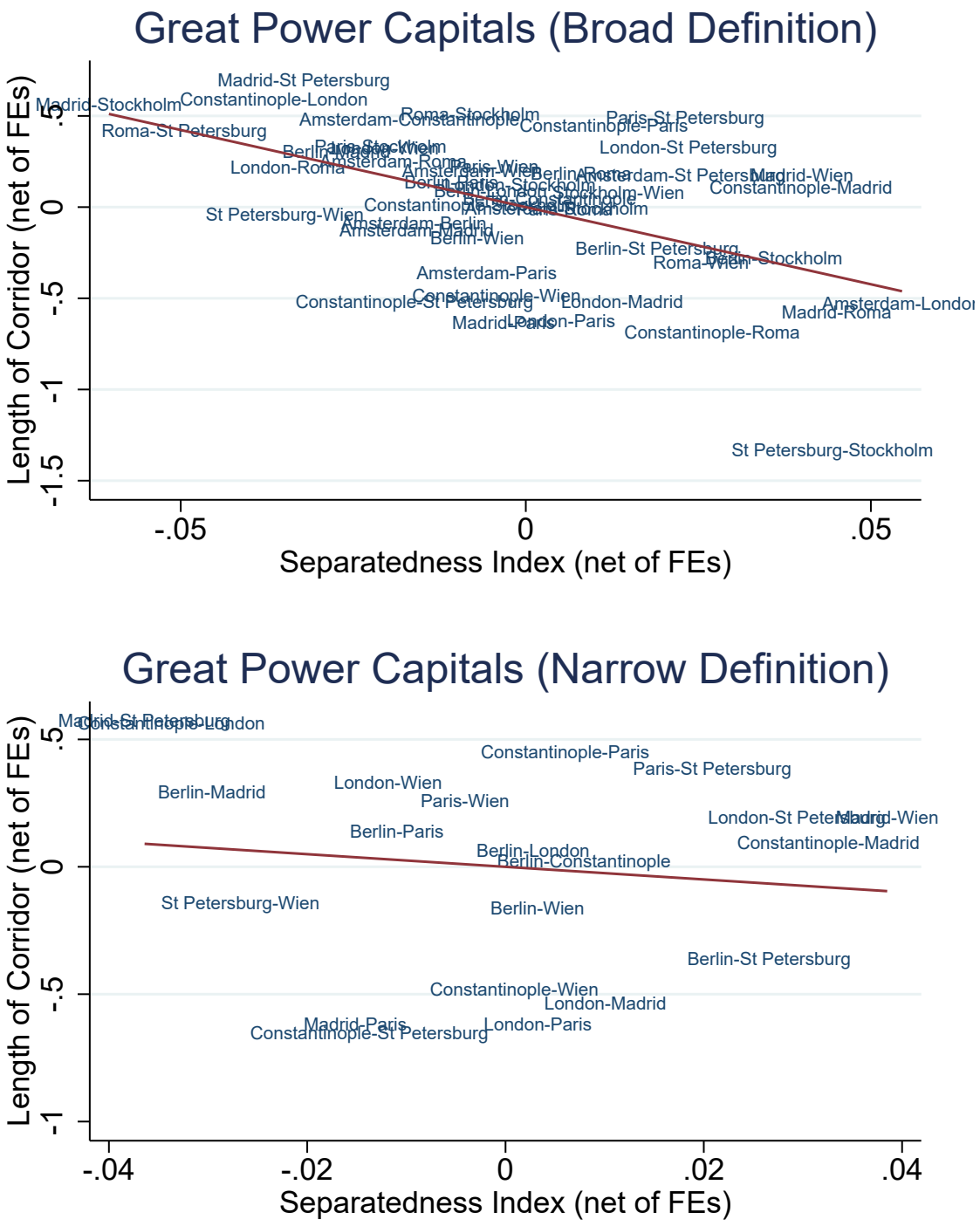

Figure A.9: Plots showing the negative relationship between geodesic distance and separatedness for Great Power capitals, based on both a narrow definition, using the same set of Great Power capitals as in the battle analysis, and a broader definition including Stockholm and Amsterdam.

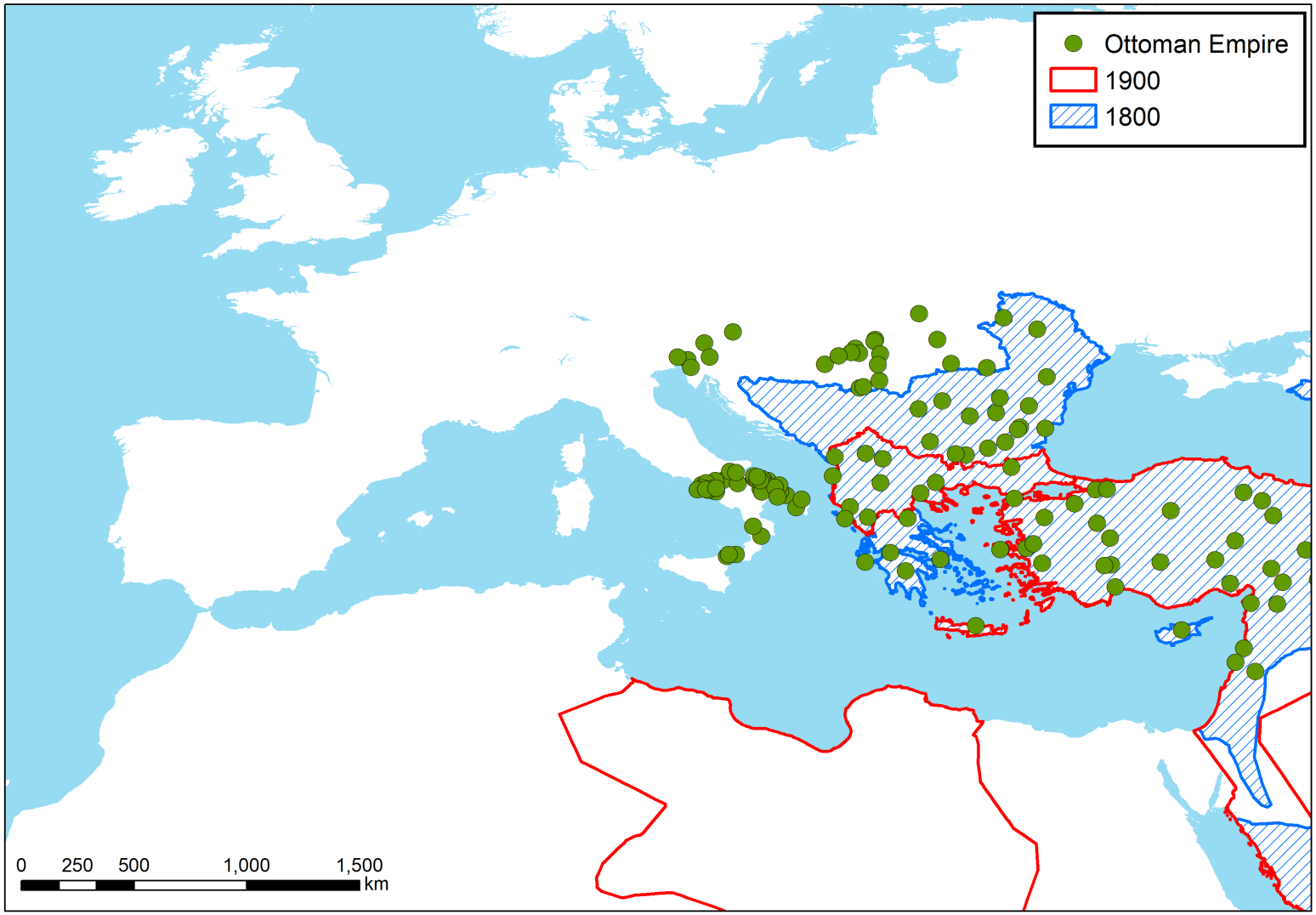

Figure A.10: As similar map as in Figure 4, but showing the actual borders of the Ottoman Empire in both 1800 and 1900.

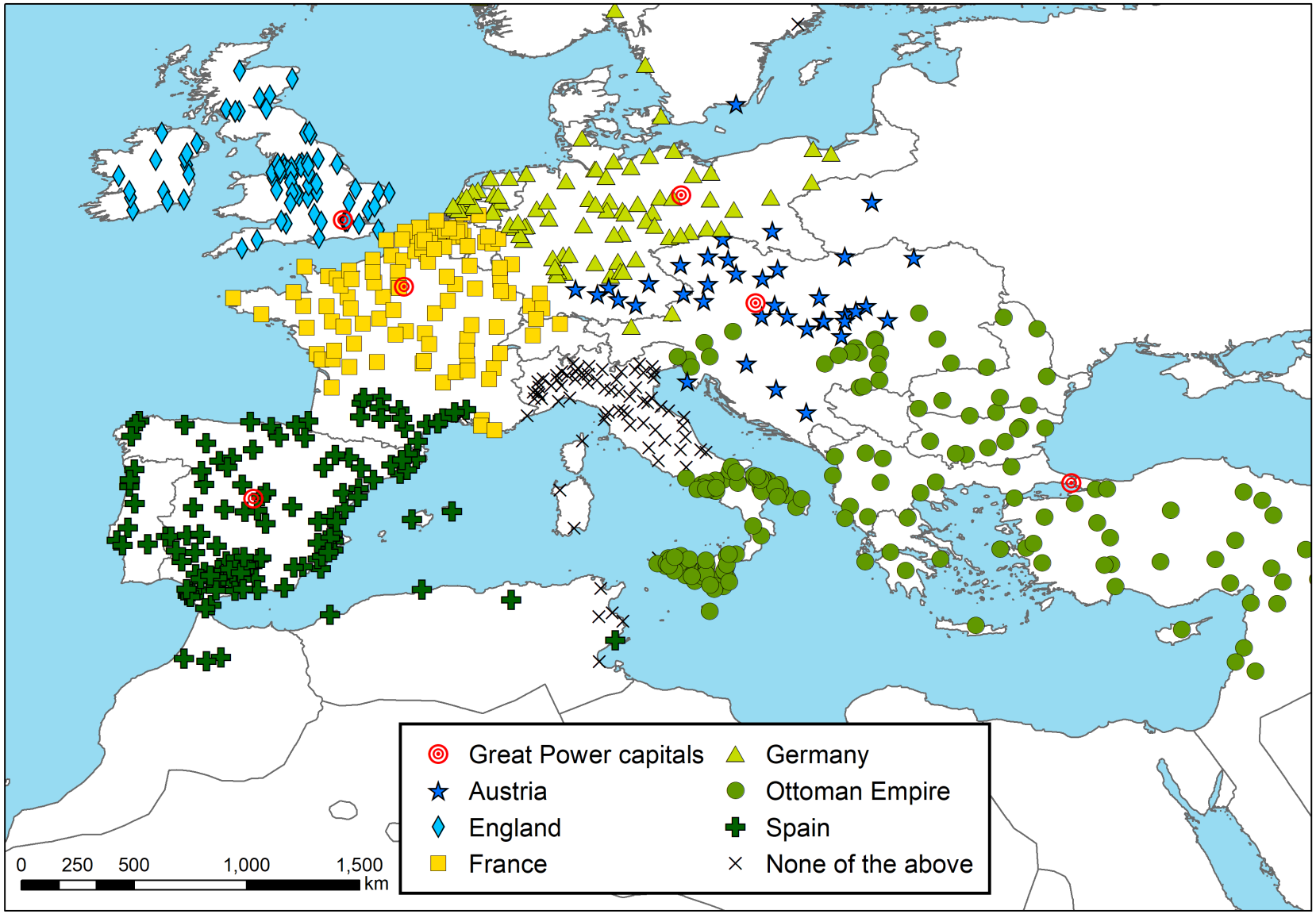

Figure A.11: The same map as in Figure 4, but using 0.1 (instead of the benchmark 0.15) as the predicted probability threshold when determining which cities belong to a Great Power and which do not.

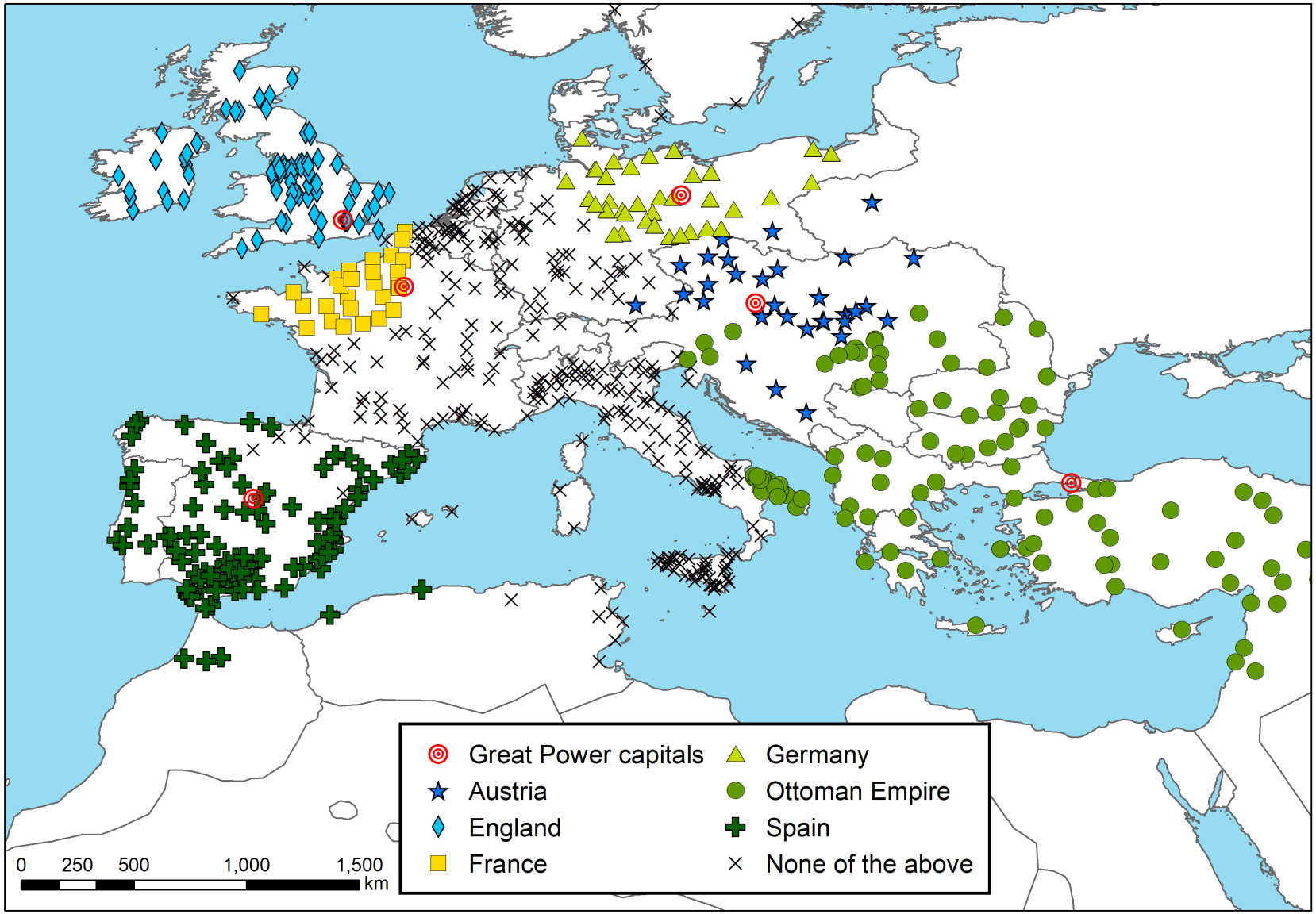

Figure A.12: The same map as in Figures 4 and A.11, but using 0.2 as the predicted probability threshold when determining which cities belong to a Great Power and which do not.

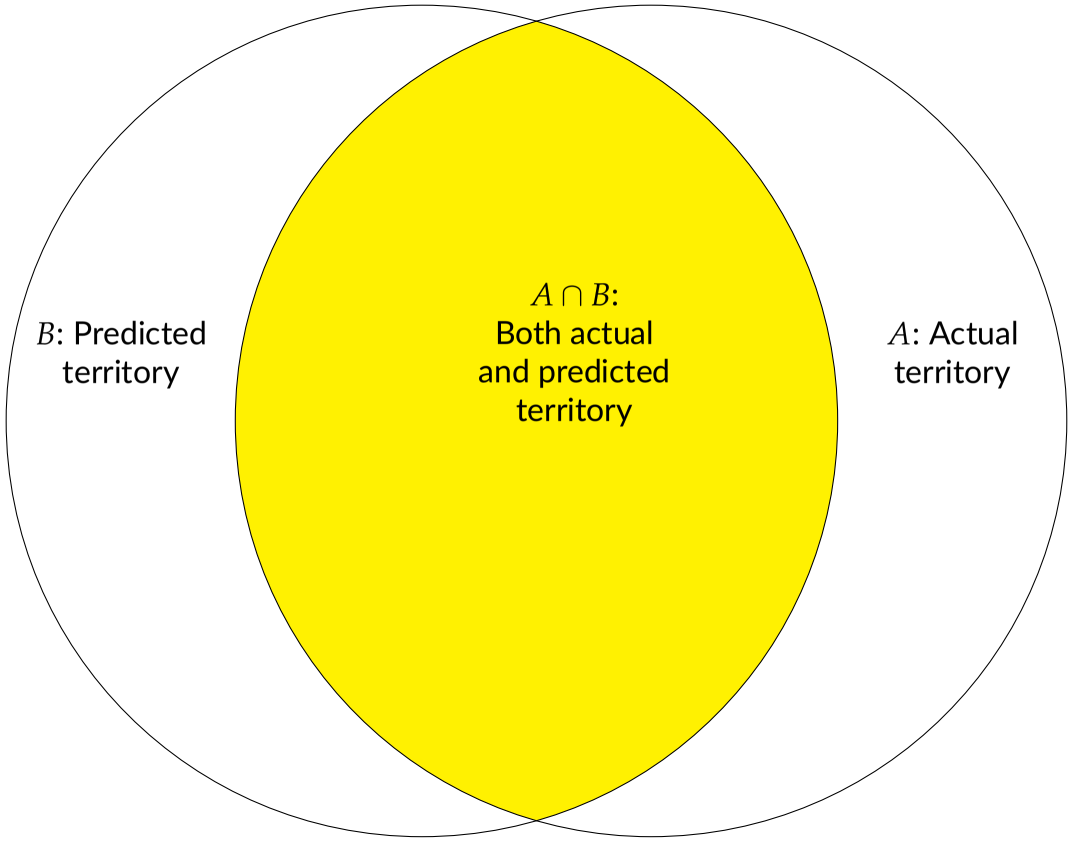

Figure A.13: Illustration of how the overlap ratio is calculated.

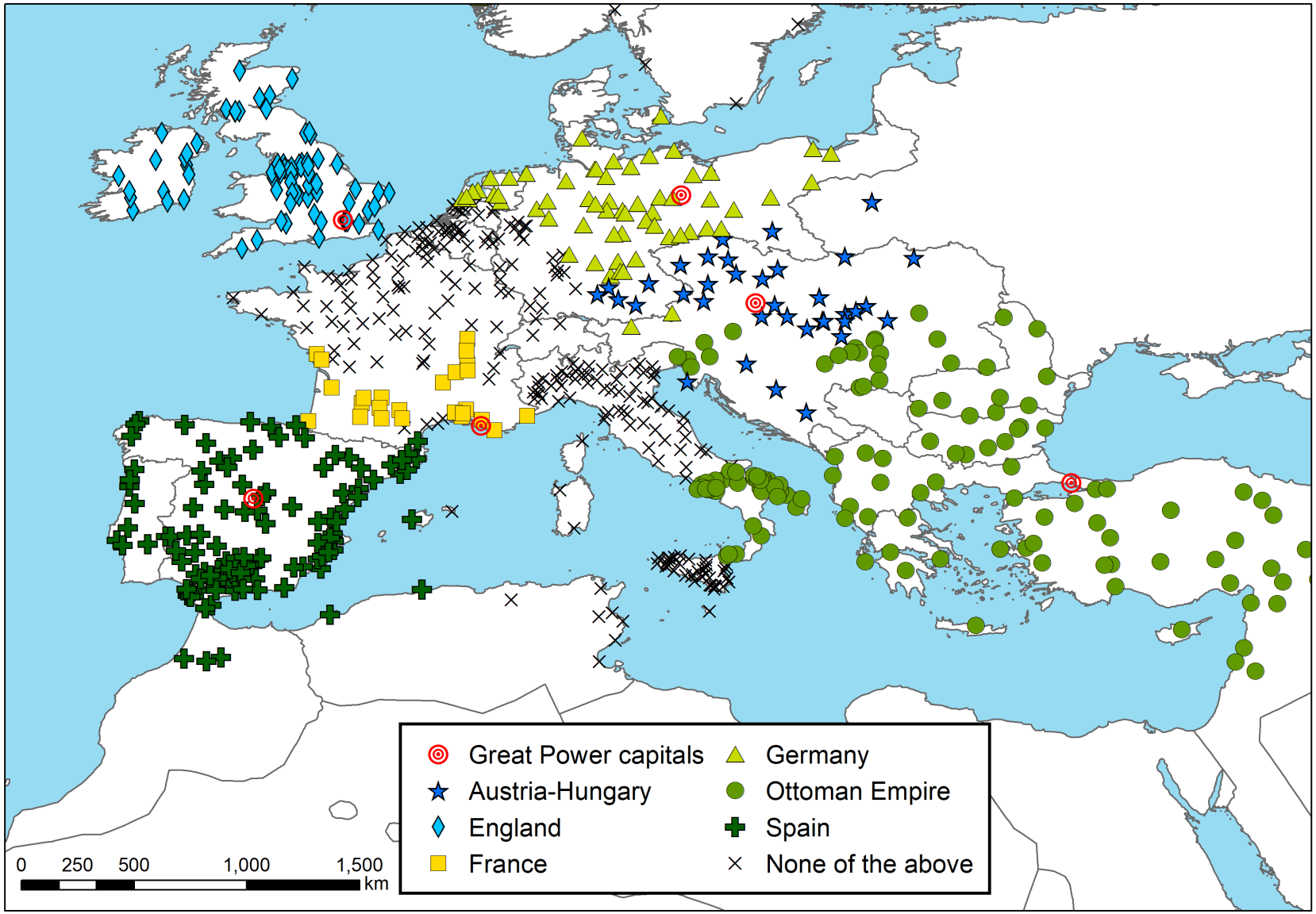

Figure A.14: The same map as in Figure 4, but changing France's capital from Paris to Marseille, keeping all other Great Power capitals unchanged.